

# Organic & Biomolecular Chemistry

Accepted Manuscript



This is an *Accepted Manuscript*, which has been through the Royal Society of Chemistry peer review process and has been accepted for publication.

*Accepted Manuscripts* are published online shortly after acceptance, before technical editing, formatting and proof reading. Using this free service, authors can make their results available to the community, in citable form, before we publish the edited article. We will replace this *Accepted Manuscript* with the edited and formatted *Advance Article* as soon as it is available.

You can find more information about *Accepted Manuscripts* in the [Information for Authors](#).

Please note that technical editing may introduce minor changes to the text and/or graphics, which may alter content. The journal's standard [Terms & Conditions](#) and the [Ethical guidelines](#) still apply. In no event shall the Royal Society of Chemistry be held responsible for any errors or omissions in this *Accepted Manuscript* or any consequences arising from the use of any information it contains.

## REVIEW

## "AND" luminescent "reactive" molecular logic gates: a gateway to multi-analyte bioimaging and biosensing

Cite this: DOI: 10.1039/x0xx00000x

Anthony Romieu,<sup>a,b</sup>Received 00th January 2012,  
Accepted 00th January 2012

DOI: 10.1039/x0xx00000x

www.rsc.org/

This review outlines examples that illustrate a recent and highly innovative concept in the field of (bio)molecular sensing, namely the simultaneous multi-analyte detection using "reactive" luminescent probes that are able to produce an optical signal only in response to multiple (bio)chemical inputs and through covalent chemical reactions with target (bio)analytes. Unlike conventional "AND" molecular logic gates based on supramolecular photochemical mechanisms, these unusual "smart" optical (bio)probes are suited tools to track the rise and fall of a wider range of biologically relevant analytes, in complex media and with higher selectivity. The potential utility of this concept for *in vivo* molecular imaging and possible solutions to adapt the described luminogenic processes to far-red or NIR emitters, is also discussed.

### Introduction

In the past decade, the scope of luminescent biosensing and bioimaging research has dramatically increased, thus finding numerous applications in diagnostic (*in vitro* or *in vivo*), enzyme biotechnology, environmental monitoring, food safety and forensic sciences. This tremendous development was promoted by the recent and rapid emergence of advanced chemical tools known as activatable or "smart" optical (bio)probes. If properly designed, these synthetic probes should exhibit no signal until they interact (and/or react) with their target (bio)analyte, reducing the level of background luminescence (fluorescence or bio- or chemiluminescence) and potentially endowing them with greater sensitivity. Their powerful ability to offer greater temporal and spatial sampling capability is another attractive and valuable feature. Various photophysical processes such as photo-induced electron transfer (PeT), photo-induced proton transfer and resonance energy transfer (BRET, CRET, FRET or through-bond energy transfer, TBET), or the direct change of  $\pi$ -conjugated systems (CCS) induced by (bio)chemical reactions, are routinely used to design luminogenic probes suitable for the selective detection of a single (bio)analyte in a more or less complex (biological) matrix. Among the wide range of fluorogenic probes currently available, those based on an irreversible chemical reaction in which the (bio)analyte acts either as a reactant or a catalyst, are being increasingly put forward because of their rapid response, high sensitivity, and

excellent selectivity. They are named reaction-based fluorescent probes, fluorescent chemodosimeters or pro-fluorophores, and have been the subject of several comprehensive reviews. In order to develop multi-analyte detection technologies, some academic research groups are now exploring alternative "reactive" luminogenic probes which are able to produce a detectable signal only in response to multiple (bio)chemical inputs (*vide infra*). This means that two or three targeted (bio)analytes must work in tandem or in a sequential manner to convert the probe into a luminescent product ("turn-on" emission response) or to induce a dramatic shift in its excitation/emission profiles (ratiometric response). Ideally, these "AND" molecular logic gates should make it possible to provide an alternative to serial measurements of single (bio)analytes in either the same (biological) sample at different times or two (or more) different (biological) samples in tandem. It should also facilitate the monitoring of multiple biomolecular events leading to a common disease pathology, to obtain optimal predictive accuracy for illness diagnosis and prognostication. The field of "AND" logic gates based on small molecules with chemical inputs and luminescence output has been the subject of numerous studies but still remains limited to fluorescent chemosensors that rely on non-covalent and reversible interactions with the target analytes that perturb photophysical processes within the system (known as supramolecular photochemical mechanisms). Therefore, these molecular devices can only be used to detect a limited number of analytes including  $H^+$ , metal cations and anions. To

overcome these limitations, the development of logic gates based on biomacromolecules (proteins and nucleic acids) and enzymes was also regarded. In particular, nucleic acid-based logic gates utilising functional oligonucleotides such as DNazymes which are DNA molecules possessing catalytic activity, and nucleic acid aptamers, which selectively bind to target molecules with affinity rivalling that of protein antibodies, have been successfully constructed to emulate Boolean operations such as "AND", "OR", "XOR" and "NOR".<sup>16</sup>

Herein, we outline the recent development of reaction-based molecular probes used for the simultaneous detection of two or three distinct (bio)analytes. Two main strategies for constructing this kind of luminogenic probes, including (1) the conversion of conventional fluorogenic dyes into pro-fluorophores having several distinct reaction sites, and (2) the internal construction of a bioluminophore/fluorophore scaffold controlled by the target (bio)analytes, are summarised. Also, only luminogenic probes leading to the release/formation of a single optical reporter are focused, with excluding FRET donor-acceptor systems that are able to respond to several distinct analytes with different sets of fluorescence signals.<sup>17</sup> The merits and limitations of the probes and possible improvements to be made in their rational design, are also discussed.

### Pro-fluorophores combining several distinct reaction sites

Among the numerous chemical reactions implemented in the context of single analyte-sensitive fluorogenic probes, few of them have already been used to develop "turn-on" fluorescent sensing platforms for simultaneous detection of multiple analytes in a biological environment. Indeed, the main difficulty associated with this multi-analyte fluorogenic approach relates to the selection of a combination of two (or more) biocompatible reactions which are fully orthogonal among themselves and easily applied to a single fluorescent scaffold. All examples of such integrated molecular "AND" logic gates currently available in the literature, have been published during the last two years. In this section, we describe them focusing on both the reaction types combinably used for the chemoselective (bio)sensing of two or three different analytes simultaneously and the proposed mechanisms to interpret "turn-on" or ratiometric fluorescence response of these probes. Possible improvements of these promising organic reaction-based strategies, especially through their extension to more sophisticated fluorophores (*i.e.*, those exhibiting valuable spectral features in the far-red or NIR region)<sup>18</sup> other than conventional BODIPY, coumarin and xanthene dyes, are also briefly described.

**Nucleophilic addition and protonation-deprotonation equilibrium.** Glass and co-workers recently devised tunable fluorescent molecular logic gates with potential applications to neuronal imaging.<sup>19</sup> At first, they reported a dual-analyte

fluorescent chemosensor (ExoSensar 517, **ES517**) for the direct visualization of neurotransmitters released upon exocytosis. This reaction-based fluorescent probe is able to selectively label primary amine neurotransmitters (especially, glutamate, Glu) through the formation of an iminium ion (carbonyl addition followed by dehydration) and allows for direct visualization of only active neurotransmitters released in the synaptic cleft in taking advantage of the pH gradient between the inside and outside of the synaptic vesicle (pH change from 5.0 to 7.4). The implementation of such a sensing mechanism was achieved using 7-amino-4-phenylcoumarin as fluorophore. Introduction of a formyl group in position 3 of the coumarin scaffold and conversion of its 7-NH<sub>2</sub> group into a sulfamide derivative easily deprotonable at physiological pH (pK<sub>a</sub> value close to 6), have led to a fluorogenic probe reactive toward both glutamate and hydroxide anions. In its native molecular form (Figure 1), **ES517** fluoresces *via* an intramolecular charge transfer (ICT) process from the moderate electron-donating sulfamide moiety to the electron-withdrawing aldehyde group. Both glutamate binding and sulfamide deprotonation enhance the charge transfer across the  $\pi$ -system of the fluorophore, resulting in large bathochromic shifts in both the absorption and emission profiles (Abs/Em maxima 458/514 nm for **C** compared to the blue-shifted absorption maxima of other forms clearly displayed in spectral curves. However, their emission maxima are not accurately reported within the publication). Thus, the excitation of the sensor (form **C**) at the highest wavelength of absorption (typically at 488 nm) should enable the visualization of only the "active" neurotransmitters in the synapse. Conversely, unbound sensor molecules (form **B**) would not be visualized as they absorb at a shorter wavelength (Abs maximum 428 nm for **B**). Sensing mechanism of **ES517** may be summarised as follows (Figure 2): in the cytosol, weakly fluorescent form is predominant due to the neutral pH and relatively low concentration of amines. When **ES517** enters the vesicle, it binds to the neurotransmitter whose the concentration is particularly high, to produce iminium ion **A**. Form **A** would have marginal electron transfer and weak fluorescence since its sulfamide moiety is a weak donor. Upon exocytosis, the bound complex enters the synaptic cleft, becomes deprotonated (form **C**), and produces a marked fluorescence increase due to the enhanced ICT. At present, validation of this unusual ICT-based ratiometric probe was only achieved through *in vitro* fluorescence assays and under conditions mimicking exocytosis. Reaction of 20  $\mu$ M of **ES517** with a saturating amount of primary amine (300 mM for glutamate, GABA and glycine and 100 mM for aromatic neurotransmitters namely norepinephrine, dopamine and serotonin) and pH adjustment from 5.0 to 7.4, produces a fluorescence enhancement at 517 nm by factors of 10-12 for non-aromatic neurotransmitters and 1.5-5.5 for those bearing an aromatic core. For these latter neuroanalytes, it is assumed that their electron-rich aromatic group (catechol or 5-hydroxyindole) promotes fluorescence quenching through reductive PeT process. Despite these promising results, some improvements have to be made to this reaction-based fluorescent probe in particular by increasing the

brightness of the fluorescent sensor-glutamate complex and possibly by red-shifting its excitation/emission profiles, aimed at meeting the challenge of high resolution imaging of neurotransmitter secretion in the brain. In the continuation of this first study, the same group has recently reported a series of three-input "AND" fluorescent molecular logic gates for directly imaging the corelease of glutamate and zinc(II) cation from glutamatergic secretory vesicles.<sup>20</sup> Concomitant detection of these two analytes is particularly relevant to gain insights into the mechanisms underlying neurotransmitter dysregulation and the progression of neurodegenerative diseases without altering synaptic activity. As for the previous example, these "reactive" probes are based on a 3-formylcoumarin scaffold which is able to form an imine with glutamate. This condensation reaction leads to the formation of a multidentate ligand fused to the coumarin ring and able to readily coordinate Zn(II) cation. The 7-OH group (pKa value close to 6) imparts pH-sensitivity which acts as the final switch for a "turn-on" fluorescence response (Figure 3). Finally, methyl groups are appended to the coumarin scaffold to red-shift and optimize the absorption/emission maxima of the probe (red-shift of ~10 nm with each additional methyl group). Even the sensors **1a-d** can be regarded as structural analogues of **ES517**, the changing of the pH-sensitive group and the removal of phenyl substituent in position 4 dramatically affect the fluorescence sensing mechanism. Indeed, at physiological pH, 3-formyl-7-hydroxycoumarin derivatives **1a-d** are blue fluorescent emitters (emission maximum in the range 460-480 nm) upon excitation at 416-440 nm (however, their quantum yields were not determined and are not reported within the publication). When the coumarin-based probe penetrates the zinc-containing secretory vesicles, reaction with glutamate, subsequent binding of Zn(II) cation and acidic environment lead to a sensor-glutamate-zinc bound complex which exhibits a moderate blue fluorescence upon excitation at a shorter wavelength (380-395 nm depending on the methyl-substitution pattern of coumarin). Upon exocytosis, this Zn(II) complex is released within the synaptic cleft, deprotonation of its phenol group occurs and remarkable red-shift of excitation maximum (~50 nm) and fluorescence enhancement by factors of 6-11 (depending on the methyl-substitution pattern of coumarin) are observed. Validation of these three-input sensors was again achieved through *in vitro* fluorescence assays, using high concentrations of glutamate and zinc(II) salt (typically found in glutamatergic vesicles) and under pH conditions mimicking exocytosis. The major drawback of this sensing approach is that the unreacted probe (e.g., compound **1c**) acts as a single-input "YES" molecular logic gate because a substantial fluorescence signal is obtained when the pH is increased from 5.0 to 7.4 in the lack of glutamate and/or Zn(II) cation (Figure 4). However, the authors claim that this unbound sensor is chargeless and would not accumulate within acidic secretory vesicles, but would instead be washed away during preimaging cell preparation. To abolish native fluorescence of **1a-d**, a further functionalisation of its position 8 with the di-(2-picolyl)amine (DPA) Zn(II)-chelating moiety and acetylation of its phenol group could be regarded

(Figure 5).<sup>21</sup> Indeed, as recently demonstrated by Lippard and co-workers with a fluorescein-based Zn(II) sensor of the Zinpyr (ZP) family (**DA-ZPI-TPP**), the presence of an acetyl group provides complete fluorescence quenching that is rapidly reversed on exposure to Zn(II), the Lewis acidity of which mediated hydrolysis of the ester group to afford a large, rapid, zinc-induced fluorescence response.<sup>22</sup> Furthermore, the use of an analogue of Fisher's base aldehyde derived from 2,4-diformylphenol as latent fluorescent platform may be an effective way to implement this promising multi-analyte sensing approach to a spectral range more suitable with neuronal imaging applications (Figure 6).

**Metal-catalysed reaction and nucleophilic addition-elimination.** Simultaneous detection of two reactive analytes namely mercury(II) cation and hydrogen peroxide (H<sub>2</sub>O<sub>2</sub>), known to play vital roles in the environment and in health, was recently achieved by Churchill and co-workers.<sup>23</sup> They designed the "turn-on" fluorogenic probe **2** based on a bis(dimethylthiocarbamate)-caged fluorescein whose deprotection involves two distinct reactions occurring sequentially: (1) desulfurization reaction induced by thiophilic Hg(II) cation and leading to conversion of the thiocarbonyl group to the carbonyl one and (2) deprotection by H<sub>2</sub>O<sub>2</sub> through an addition-elimination process (Figure 7).<sup>24</sup> This fluorescein-based probe was readily prepared by reaction of fluorescein with *N,N*-dimethyl-thiocarbamoyl chloride. Validation of the claimed tandem sensing mechanism was done through *in vitro* fluorescence assays performed under simulated physiological conditions (20 mM HEPES/DMSO 8 : 2, pH 7.4). First, metal ion screening involving **2** was assayed with a large excess (660 equiv) of Ca(II), Cd(II), Co(II), Cu(II), Fe(II), Mg(II), Mn(II), Pb(II), Zn(II), Ni(II), Ag(I) and Hg(II) respectively: a dramatic 50-fold increase in the fluorescence emission intensity at 520 nm with Hg(II) was found over other metals except for thiophilic Ag(I) (a 10-fold increase in fluorescence emission intensity was obtained with this monovalent cation metal). This premature fluorescence unveiling is explained by the fact that Hg(II)-induced desulfation process is combined with the deprotection of one thiocarbonyl group leading to emissive mono-carbamate intermediate **3'**. Fortunately, further addition of the same excess amount of second targeted analyte namely H<sub>2</sub>O<sub>2</sub> leads to a higher increase in fluorescence (a 100-fold increase relative to that for the starting probe **2**). Thus, this fluorogenic system can be interpreted as an "AND" logic gate for Hg(II) and H<sub>2</sub>O<sub>2</sub>. However, upon its "pre-activation" with Hg(II), probe **2** exhibits a very moderate selectivity for H<sub>2</sub>O<sub>2</sub> over other reactive oxygen species (ROS) such as *meta*-chloroperbenzoic acid (*m*-CPBA), KO<sub>2</sub> and NaOCl. Finally, the biocompatibility of this reaction-based approach was demonstrated through an assays using living neuronal cells. SH-SY5Y neuroblastoma cells treated with a Hg(II) salt and H<sub>2</sub>O<sub>2</sub>, were incubated with probe **2**. Fluorescence confocal microscopy reveals the same pattern of responses than that observed *in vitro* (Figure 8). Interestingly, this fluorogenic dual-reagent-mediated phenol deprotection strategy can also be



applied to red-emitting naphthofluorescein derivatives, thereby facilitating dual bioimaging of Hg(II) and H<sub>2</sub>O<sub>2</sub> in complex biological media (Figure 9).<sup>25</sup> The best way to improve the selectivity of bis-caged-fluorescein probes (such as **2**) toward two distinct analytes such as Hg(II) and H<sub>2</sub>O<sub>2</sub>, is no doubt based on the implementation of two different reactions each one triggered by a single analyte but both leading to the phenol release. Building on previous works on luminescent chemodosimeters for Hg(II) cation or H<sub>2</sub>O<sub>2</sub>,<sup>26</sup> it is fairly easy to design a fluorescein-based probe whose the phenolic hydroxyl groups would, for instance, be replaced by alkynyl ether and pinacol boronate moieties. Indeed, alkyne ethers readily react with Hg(II) cation according to an oxymercuration-elimination process whereas H<sub>2</sub>O<sub>2</sub> is known to promote transformation of monoboronates to phenols through an oxidative cleavage reaction. Interestingly, this fluorogenic sensing strategy based on two distinct sequential reactions affecting the same quenching moiety, has been recently applied to a mitochondria-targetable fluorescent probe for dual-channel nitric oxide (NO) imaging assisted by intracellular biothiols (cysteine or glutathione (GSH), Figure 10).<sup>27</sup> Introduction of the *ortho*-phenylene diamine (OPD) moiety in position 9 of pyronin B has led to probe **4** whose fluorescence is completely abolished by PeT process. NO is known to react specifically with OPD to form a triazole ring, and therefore leads to the quantitative conversion of **4** into fluorescent benzotriazole-pyronin dye **5** (Abs/Em maxima 591/616 nm). Since the benzotriazole unit is a good leaving group, this latter fluorophore subsequently reacts with GSH or cysteine through a S<sub>N</sub>Ar-type reaction to give a red-emitting thiopyronin dye **6**. In the case of cysteine, a further rearrangement reaction takes place to provide green-emitting aminopyronin dye **7**. Therefore, pro-fluorophore **4** is able to sequentially react with two distinct bioanalytes but does not behave as a "AND" molecular logic gate.

**Metal complexation and oxidation reaction.** Concomitant detection of mercury(II) cation and a ROS, namely the superoxide anion radical O<sub>2</sub><sup>•-</sup> was also carried out through a dramatically different chemosensing approach based on the fluorescence exaltation of a *meso*-thienyl BODIPY dye whose the thia-heterocycle is substituted with one or two 2-pyridyl-sulfide arms.<sup>28</sup> The binding receptor [S<sub>thi</sub>,N<sub>py</sub>] or [S<sub>thi</sub>,N<sub>py</sub>,N<sub>py</sub>] of such PeT-based probes acts as a quencher due to its high electron-donating ability, until coordination of Hg(II) cation. In addition to suppressing the PeT process, metal chelation leads to enhanced sterical rigidity of the *meso*-aryl group which may further help fluorescence recovery. Sulfide moieties are reactive toward O<sub>2</sub><sup>•-</sup> radical anion and their oxidation is an effective and complementary way to minimise the reductive PeT effect of the Hg(II)-chelating *meso*-aryl substituent (Figure 11). The BODIPY-based probes **10** and **11** were prepared from 2,4-dimethylpyrrole and 3-thiophenecarboxaldehyde **8** or **9** using a standard one-pot protocol. Interestingly, the two aryl-aldehydes functionalised with either one or two 2-pyridyl-sulfide arms were obtained through a single copper-catalysed cross-coupling

reaction between 2,5-dibromo-3-thiophene carboxaldehyde and 2-mercaptopyridine, in 45% and 13.5% yield respectively. *In vitro* validation of **10** and **11** was performed in a mixture CH<sub>3</sub>CN/H<sub>2</sub>O (7 : 3, v/v), according to a methodology identical to that use for the bis(dimethylthiocarbamate)-caged fluorescein **2** (*vide supra*). Selective coordination of Hg(II) cation through the formation of 1:1 stoichiometry complexes, was clearly demonstrated through UV-vis absorption measurements. Only addition of this divalent cation (in its perchlorate salt form) causes the absorbance band to split into two components and the second local maximum centered at 532 nm is ~25 nm red-shifted compared to the absorption maximum of unchelated probes. The residual fluorescence emission of probes **12** and **13** at 524 nm (QY ~2% in CH<sub>3</sub>CN/H<sub>2</sub>O, 7 : 3, v/v) slightly decreases but since no molar extinction coefficients for Hg(II).probe complexes are reported, it is difficult to conclude that quenching occurs especially through an enhanced spin-orbit coupling. Further addition of KO<sub>2</sub> leads to a dramatic green fluorescence enhancement of the mercury(II) chelate-probes **12** and **13** (a ~25-fold increase in emission intensity at 524 nm was obtained). Dual addition of analytes in reverse order: probe + O<sub>2</sub><sup>•-</sup> + Hg(II), leads to a similar strong "turn-on" fluorescence response. Such fluorogenic reactivity toward O<sub>2</sub><sup>•-</sup> is also observed with unchelated probes **10** and **11** but a (lower) ~7-fold increase in emission intensity is obtained. This set of results supports that pro-fluorescent BODIPY dyes **10** and **11** act as two-input "AND" logic gates for tandem Hg(II) and O<sub>2</sub><sup>•-</sup> detection (Figure 12). Moreover, a satisfying selectivity for O<sub>2</sub><sup>•-</sup> over other ROS was obtained because only *m*-CPBA also leads to a significant fluorescence increase of probes **10** and **11** but nevertheless six times lower than observed with superoxide anion radical. To elucidate the reaction pathway giving this excellent "turn-on" signal in the presence of both analytes, authentic samples of mono- and di-oxidized forms of probe **10** (*i.e.*, sulfoxide **18** and sulfone **19**) were prepared by treatment with *m*-CPBA and isolated by silica gel column chromatography in 49% and 18.5% yield respectively. These two compounds are strongly fluorescent (QY = 87% and 77% respectively), but exhibit no optical response to Hg(II) cation. This means that for probes **10** and **11**, a long-lasting (but not isolable) oxidised species giving a signal from the superoxide is neither the sulfoxide nor the sulfone (see compounds **14** and **15** or **16** and **17** in Figure 11). Among the numerous intermediates potentially generated in the oxidation of organic sulfides, dioxathirane, persulfoxide or sulfide radical ion superoxide pair may be involved in this fluorogenic process.<sup>29</sup> Both biocompatibility and efficacy of the superoxide-mediated sulfide oxidation reaction and the lack of cytotoxicity for this novel class of BODIPY-based probes were finally demonstrated in the context of neuroblastoma cells and a moderate fluorescence response was obtained with the probe **11** + ROS only (not Hg(II)). However, a further extension to Hg(II) imaging in live cells seems to be problematic due to the competitive chelation action of certain amino acids such as cysteine. Thus, it may be irrelevant to apply this unusual tandem chelation/oxidation fluorogenic reaction to red/NIR

region BODIPY dyes<sup>30</sup> more appropriate for bioimaging applications.

### ***In situ* formation of bioluminophore/fluorophore scaffold mediated by two distinct (bio)analytes**

The multi-analyte detection strategy shown in the examples above is currently limited by the need to use fluorophores that exhibit intrinsic fluorogenic behavior, typically obtained through the reversible (bio)chemical modification of an aniline or a phenol moiety present in their core structure. Thus, such approach may be applicable for a limited number of fluorophores whose spectral features in the visible region are often not compatible with biosensing/bioimaging in complex biological media: 7-amino-/7-hydroxycoumarins, conventional xanthene dyes (*e.g.*, (naphtho)fluorescein, rhodamine 110, rhodols, ...) or precursors that are able to generate a large  $\pi$ -conjugated system upon reaction with a single analyte (typically an intramolecular cyclisation reaction, Figure 13, top). To overcome this limitation, a sophisticated alternative would be to use two non-fluorescent precursors that are sensitive/reactive toward targeted (bio)analytes and will then be able to readily react among themselves (typically a bimolecular process) and under mild conditions, to *in situ* generate a luminescent compound (Figure 13, bottom). To the best of our knowledge, self-assembling fluorescent molecular sensors based on multistep reaction cascades, initiated by two (or more) distinct analytes have not yet been reported in the literature. However, recent achievements in the field of molecular (bio)sensing focused on development of novel rapid, efficient (and possibly biocompatible) fluorogenic reactions triggered by a single (bio)analyte and leading to *in situ* assembly of a fluorophore, will undoubtedly allow to fill this gap.<sup>31</sup> The majority of these works display a fluorimetric assay based on the conversion of a non-fluorescent phenolic derivative to a highly fluorescent (imino)coumarin product, usually through a specific cyclisation reaction triggered by the reactive analyte (Figure 14).<sup>32</sup> Since, 7-amino-/7-hydroxycoumarins are known to be fluorogenic dyes (*vide supra*), one would assume that the further functionalization of the (imino)coumarin-precursor with an aniline or a phenol moiety masked by a trigger-recognition unit reactive toward a second distinct (bio)analyte, could easily lead to reaction-based probes acting as "AND" fluorogenic logic gates (Figure 15). Interestingly, alternative reactions such as aldolisation-elimination<sup>33</sup> (or related reactions)<sup>34</sup>, Mannich cyclisation<sup>35</sup> (or related intramolecular addition-elimination reactions)<sup>36, 37</sup>, phenylogous Vilsmeier-Haack<sup>38</sup>,  $S_EAr$ <sup>39, 40</sup> or tandem phenol oxidation-Michael addition<sup>41</sup> have been also implemented to detect various (bio)analytes including G-quadruplex DNA structures, penicillin G acylase (PGA), monoamine oxidases (MAO A and B), sarin mimics, NO and peroxyxynitrite (OONO<sup>•</sup>) through the formation of cyanine, pyronin B, pyrazino-benz[e]indole, pyrrolocoumarin, diazachrysen and resorufin fluorescent scaffolds respectively (Figure 16). One can also point out other fluorogenic reactions whose the mechanism underlying *in situ* formation of the

fluorescent scaffold remains uncertain. One good example is the conversion of 6-nitroquinoline into a fluorescent helicene named pyrido[3,2-*f*]quinolino[6,5-*c*]cinnoline 3-oxide, under hypoxic conditions (Figure 17).<sup>42</sup> For most of these examples, two distinct reactive sites involving in the fluorogenic "covalent-assembly" process are clearly identified within the core structure of the fluorophore precursor. Thus, it is reasonable to assume that the masking of these two reactive functionalities with bio-labile or analyte-sensitive protecting groups will lead to effective dual-analyte responsive fluorescent chemodosimeters. For instance, the design of a dual-analyte fluorogenic probe based on a mixed diaminoaryl ether scaffold with the following structural features: (1) a primary aniline substituted with a self-immolative carbamate spacer or protected as a carboxamide and (2) a tertiary aniline *para*-functionalized with a formyl group masked as an hemithioaminal or  $\alpha$ -alkoxy carbamate responsive to one of the two targeted analytes<sup>43</sup>, should enable the simultaneous detection of two (bio)chemical species, through *in situ* formation of a unsymmetrical pyronin fluorophore (Figure 18). Further extension of "covalent assembly" approach to longer wavelength fluorescent dyes (typically far-red or NIR cyanine dyes)<sup>44</sup> will also be studied to allow *in vivo* applications. However, this would imply using either an heterobifunctional cross-linker (with optimal length and geometry) or a multivalent molecular platform for grafting the two complementary fluorophore precursors in close proximity to each other and through a well-defined and controlled spatial orientation<sup>45</sup>, thus favoring the reaction rate of the fluorogenic bimolecular process. An attractive alternative could be the use of erythrocytes (red blood cells) as capture agent for both lipidated caged precursors (*i.e.*, pre-functionalized with a long alkyl chain) through strong interaction with the lipophilic membrane of these carriers. Such cell-based assembly strategy has been recently applied successfully to a pair of lipidated photo-labile prodrug (an anti-inflammatory drug covalently appended to an alkylcobalamin) and far-red emitting fluorophore (cyanine dye Cy 5.0 acting as antenna and energy donor) for applications in photo-induced drug delivery (Figure 19).<sup>46</sup>

An interesting recent development in the field of "click" chemistry, made it possible to perform concurrent *in vivo* monitoring of two distinct (bio)analytes using luciferin-based bioluminescence imaging technologies. Indeed, inspired by the Nature and after a comprehensive study of the regeneration pathway of D-luciferin (a common bioluminescent substrate for firefly luciferase) in fireflies, Rao and co-workers discovered a new, biocompatible reaction between 6-substituted 2-cyanobenzothiazole (CBT) derivatives and D-cysteine, which can be controlled by pH, redox status and hydrolytic enzyme activities to synthesize large molecules and form different nanostructures (Figure 20).<sup>47</sup> In the space of just five years, this thiol-based "click" reaction has been extensively studied and successfully applied to *in vivo* molecular imaging, through the clever design of nano-aggregation fluorescent or magnetic resonance (MR) probes for the non-invasive detection of

protease activities (furin and caspases) or for sensing reducing environment.<sup>48</sup> In 2013, Bertozzi, Chang and co-workers implemented this "click" condensation reaction to the simultaneous *in vivo* imaging of two distinct analytes namely H<sub>2</sub>O<sub>2</sub> and caspase-8 (an apoptosis-related cysteine protease).<sup>49</sup> Their strategy employs *in situ* formation of firefly luciferin from two complementary caged precursors namely "peroxy caged luciferin 2 (PCL-2)" and Z-Ile-Glu-Thr-Asp-D-Cys (IETDC) that can be unmasked through a selective reaction with the targeted ROS and protease respectively. Indeed, PCL-2 is a H<sub>2</sub>O<sub>2</sub>-responsive boronic acid probe that releases 6-hydroxy-2-cyanobenzothiazole (HCBT) through boronate oxidation to phenol followed by 1,6-elimination reaction whereas pentapeptide IETDC is a potent substrate of caspase-8 which hydrolyses the peptide bond after the aspartic acid residue to release D-cysteine. Once released, HCBT and D-Cys subsequently react together to yield luciferin *in situ*, resulting in a bioluminescent signal under the action of luciferase (Figure 21). Moreover, concomitant use of PCL-2 and IETDC *in vivo* establishes a concurrent increase in both H<sub>2</sub>O<sub>2</sub> and caspase-8 activity during acute inflammation in living mice. This "self-assembly" bioluminogenic approach is therefore a powerful tool for studying simultaneous oxidative stress and inflammation processes in living animals during injury, aging and disease, and may be extended to concurrent monitoring of multiple (bio)analytes. This should be made easier by the current availability of a wide range of "activatable" luciferin-based bioluminescent probes (also known as caged luciferins) suitable to image a variety of enzymatic activities (*e.g.*, glycosylase, MAO, protease, sulfatase) and physiological states<sup>10, 50</sup>, that can serve as a relevant source of inspiration for design and synthesis of other caged luciferin precursors. Furthermore, an extension of this bioluminogenic "click" reaction to D-selenocysteine (D-Sec), will lead to the *in situ* formation of a luciferin analogue having a luminescence maximum close to 600 nm, more suited for *in vivo* imaging (Figure 20).<sup>51, 52</sup>

## Conclusions and outlook

In this feature article, I hope I have been able to demonstrate that reaction-based luminescent probes are tools well suited for devising new sensing systems for concomitant detection of several (bio)analytes at the nano-scale and within the same sample or biological medium. Contrary to more conventional "AND" molecular logic gates based on supramolecular photochemical mechanisms (commonly employed for multi-cation and/or multi-anion detection), such "lab-on-a-molecule" prototypes can be applied to a wider range of reactive (bio)analytes including biomolecules and disease-related enzymes, by judicious selection of the suitable reaction sites. This could be particularly interesting to develop innovative new diagnostic tests for diseases where the combined detection/quantification of two distinct biomarkers is preferred to avoid "false positive" results (*e.g.*, prostate cancer<sup>53, 54</sup>). Dual-controlled activatable optical (bio)probes could also be

used to achieve high target-to-background signal ratio (TBR) and thus improve the sensitivity of *in vivo* molecular imaging.<sup>55</sup> In this context, the concept of double enzymatic activation of pre-pro-fluorophores recently published by Prost and Hasserodt and applied to the simultaneous detection of  $\beta$ -D-galactosidase and leucine amino-peptidase through the release of a precipitating phenol-based fluorophore, is very relevant and promising.<sup>56</sup> Furthermore, "dual-lock" structures combining two distinct reactive/quenching groups sensitive to the same analyte, have recently emerged as valuable tools for designing reaction-based fluorescent probes with unprecedented performances (*i.e.*, selectivity and sensitivity) for single analyte sensing.<sup>57</sup> The discovery of novel biocompatible fluorogenic reactions will facilitate the design of "reactive" probes leading to *in situ* formation of fluorescent scaffolds with valuable spectral features in the NIR wavelength range, known as the "therapeutic" window<sup>58</sup>, will also contribute to this challenging goal.

## Acknowledgements

I thank the Institut Universitaire de France (IUF) and the Burgundy region ("FABER" programme, PARI Action 6, SSTIC 6 "Imagerie, instrumentation, chimie et applications biomédicales") for financial support, and Dr. Céline Péroliier for critical reading of the manuscript before publication. A special note of gratitude is also owed to Pr. P.-Y. Renard and my former co-workers from the University of Rouen for their significant contribution to the exciting research field of pro-fluorescence (including both synthetic and bioanalytical aspects): Dr. L. Louise-Leriche, Dr. S. Poupart, Dr. J.-A. Richard, Dr. Y. Meyer, Dr. V. Grandclaude, Dr. C. Massif, Dr. N. Maindrion, Dr. A. Chevalier, B. Roubinet and X. Brune.

## Notes and references

<sup>a</sup>Institut de Chimie Moléculaire de l'Université de Bourgogne, UMR CNRS 6302, Université de Bourgogne, 9, Avenue Alain Savary, 21078 Dijon, France. E-mail: [anthony.romieu@u-bourgogne.fr](mailto:anthony.romieu@u-bourgogne.fr); Fax: +33-3-80-39-61-17; Tel: +33-3-80-39-36-24. Lab homepage: <http://www.icmub.fr>  
<sup>b</sup>Institut Universitaire de France, 103 Boulevard Saint Michel, 75005 Paris, France

- (a) C. Bremer, V. Ntziachristos and R. Weissleder, *Eur. Radiol.*, 2003, **13**, 231; (b) D. Shin, N. Vigneswaran, A. Gillenwater and R. Richards-Kortum, *Future Oncol.*, 2010, **6**, 1143.
- (a) J.-L. Reymond, *Chimia*, 2001, **55**, 1049; (b) D. Wahler and J.-L. Reymond, *Curr. Opin. Biotechnol.*, 2001, **12**, 535; (c) J.-L. Reymond, *Food Technol. Biotechnol.*, 2004, **42**, 265; (d) J.-L. Reymond, V. S. Fluxa and N. Maillard, *Chem. Commun.*, 2009, 34.
- For a selected example, see: W. Jiang, S. Wang, L. H. Yuen, H. Kwon, T. Ono and E. T. Kool, *Chem. Sci.*, 2013, **4**, 3184.
- For selected examples, see: (a) A. C. Vinayaka and M. S. Thakur, *Anal. Bioanal. Chem.*, 2010, **397**, 1445; (b) H. Kwon, F. Samain and E. T. Kool, *Chem. Sci.*, 2012, **3**, 2542.
- N. Frascione, J. Gooch and B. Daniel, *Analyst*, 2013, **138**, 7279.
- (a) C.-H. Tung, *Biopolymers*, 2004, **76**, 391; (b) X. Chen, M. Sun and H. Ma, *Curr. Org. Chem.*, 2006, **10**, 477; (c) N. Johnsson and K.



- Johnsson, *ACS Chem. Biol.*, 2007, **2**, 31; (d) J. F. Lovell and G. Zheng, *J. Innov. Opt. Health Sci.*, 2008, **1**, 45.
7. For a comprehensive review, see: W. Zhang, Z. Ma, L. Du and M. Li, *Analyst*, 2014, **139**, 2641.
  8. For a comprehensive review, see: J. E. Kwon and S. Y. Park, *Adv. Mater.*, 2011, **23**, 3615.
  9. For comprehensive reviews, see: (a) M. K. Johansson and R. M. Cook, *Chem. Eur. J.*, 2003, **9**, 3466; (b) K. E. Sapsford, L. Berti and I. L. Medintz, *Angew. Chem. Int. Ed.*, 2006, **45**, 4562; (c) J. Fan, M. Hu, P. Zhan and X. Peng, *Chem. Soc. Rev.*, 2013, **42**, 29.
  10. M. A. Paley and J. A. Prescher, *MedChemComm*, 2014, **5**, 255.
  11. For a comprehensive review, see: W. Shi and H. Ma, *Chem. Commun.*, 2012, **48**, 8732.
  12. (a) G. J. Mohr, *Chem. - Eur. J.*, 2004, **10**, 1082; (b) G. J. Mohr, *Springer Ser. Chem. Sens. Biosens.*, 2004, **1**, 51; (c) G. J. Mohr, *Sens. Actuators, B*, 2005, **107**, 2.
  13. (a) H. N. Kim, M. H. Lee, H. J. Kim, J. S. Kim and J. Yoon, *Chem. Soc. Rev.*, 2008, **37**, 1465; (b) M. Beija, C. A. M. Afonso and J. M. G. Martinho, *Chem. Soc. Rev.*, 2009, **38**, 2410; (c) M. Eun Jun, B. Roy and K. Han Ahn, *Chem. Commun.*, 2011, **47**, 7583; (d) X. Chen, T. Pradhan, F. Wang, J. S. Kim and J. Yoon, *Chem. Rev.*, 2012, **112**, 1910; (e) J. B. Grimm, L. M. Heckman and L. D. Lavis, *Prog. Mol. Biol. Transl. Sci.*, 2013, **113**, 1; (f) Y. Yang, Q. Zhao, W. Feng and F. Li, *Chem. Rev.*, 2013, **113**, 192; (g) H. Zheng, X.-Q. Zhan, Q.-N. Bian and X.-J. Zhang, *Chem. Commun.*, 2013, **49**, 429; (h) X. Li, X. Gao, W. Shi and H. Ma, *Chem. Rev.*, 2014, **114**, 590.
  14. This is distinct from combinatorial luminescent molecular sensors recently highlighted by Rout *et al.*, see: B. Rout, L. Motiei and D. Margulies, *Synlett*, 2014, **25**, 1050.
  15. For selected reviews, see: (a) V. Bojinov and N. Georgiev, *J. Univ. Chem. Technol. Metall.*, 2011, **46**, 3; (b) A. P. de Silva, *Chem. Asian J.*, 2011, **6**, 750; (c) A. Prasanna de Silva, *J. Comput. Theor. Nanosci.*, 2011, **8**, 409.
  16. For a recent review, see: D.-L. Ma, H.-Z. He, D. S.-H. Chan and C.-H. Leung, *Chem. Sci.*, 2013, **4**, 3366.
  17. For a recent example, see: L. Yuan, W. Lin, Y. Xie, B. Chen and S. Zhu, *J. Am. Chem. Soc.*, 2012, **134**, 1305.
  18. For recent reviews, see: (a) J. O. Escobedo, O. Rusin, S. Lim and R. M. Strongin, *Curr. Opin. Chem. Biol.*, 2010, **14**, 64; (b) V. J. Pansare, S. Hejazi, W. J. Faenza and R. K. Prud'homme, *Chem. Mater.*, 2012, **24**, 812; (c) M. Ptaszek, *Prog. Mol. Biol. Transl. Sci.*, 2013, **113**, 59; (d) K. Umezawa, D. Citterio and K. Suzuki, *Anal. Sci.*, 2014, **30**, 327.
  19. J. L. Klockow, K. S. Hettie and T. E. Glass, *ACS Chem. Neurosci.*, 2013, **4**, 1334.
  20. K. S. Hettie, J. L. Klockow and T. E. Glass, *J. Am. Chem. Soc.*, 2014, **136**, 4877.
  21. K. P. Carter, A. M. Young and A. E. Palmer, *Chem. Rev.*, 2014, **114**, 4564.
  22. W. Chyan, D. Y. Zhang, S. J. Lippard and R. J. Radford, *Proc. Natl. Acad. Sci. USA*, 2014, **111**, 143.
  23. D. P. Murale, H. Liew, Y.-H. Suh and D. G. Churchill, *Anal. Methods*, 2013, **5**, 2650.
  24. This sequential approach was recently used for the dual chromogenic detection of hydrogen sulfide and nitric oxide, through the conversion of a bis-azidoaryl aza-BODIPY dye into the corresponding bis-phenol aza-BODIPY derivative, through a bis-aniline intermediate see: N. Adarsh, M. S. Krishnan and D. Ramaiah, *Anal. Chem.*, 2014, **86**, 9335.
  25. For selected examples that described synthesis and photophysical properties of naphthofluorescein analogues, see: (a) S. A. Hilderbrand and R. Weissleder, *Tetrahedron Lett.*, 2007, **48**, 4383; (b) E. Azuma, N. Nakamura, K. Kuramochi, T. Sasamori, N. Tokitoh, I. Sagami and K. Tsubaki, *J. Org. Chem.*, 2012, **77**, 3492.
  26. (a) F. Song, S. Watanabe, P. E. Floreancig and K. Koide, *J. Am. Chem. Soc.*, 2008, **130**, 16460; (b) B. C. Dickinson, C. Huynh and C. J. Chang, *J. Am. Chem. Soc.*, 2010, **132**, 5906.
  27. Y.-Q. Sun, J. Liu, H. Zhang, Y. Huo, X. Lv, Y. Shi and W. Guo, *J. Am. Chem. Soc.*, 2014, **136**, 12520.
  28. A. P. Singh, D. P. Murale, Y. Ha, H. Liew, K. M. Lee, A. Segev, Y.-H. Suh and D. G. Churchill, *Dalton Trans.*, 2013, **42**, 3285.
  29. N. Sawwan and A. Greer, *Chem. Rev.*, 2007, **107**, 3247.
  30. (a) H. Lu, J. Mack, Y. Yang and Z. Shen, *Chem. Soc. Rev.*, 2014, **43**, 4778; (b) Y. Ni and J. Wu, *Org. Biomol. Chem.*, 2014, **12**, 3774.
  31. E. V. Anslyn, *J. Am. Chem. Soc.*, 2010, **132**, 15833.
  32. (a) W. Jiang and W. Wang, *Chem. Commun.*, 2009, 3913; (b) T.-I. Kim, M. S. Jeong, S. J. Chung and Y. Kim, *Chem. - Eur. J.*, 2010, **16**, 5297; (c) T.-I. Kim, H. Kim, Y. Choi and Y. Kim, *Chem. Commun.*, 2011, **47**, 9825; (d) I. Kim, D. Kim, S. Sambasivan and K. H. Ahn, *Asian J. Org. Chem.*, 2012, **1**, 60; (e) J. Park and Y. Kim, *Bioorg. Med. Chem. Lett.*, 2013, **23**, 2332; (f) J. Kim, J. Park, H. Lee, Y. Choi and Y. Kim, *Chem. Commun.*, 2014, **50**, 9353; (g) P. Hou, S. Chen, H. Wang, J. Wang, K. Voitchovsky and X. Song, *Chem. Commun.*, 2014, **50**, 320.
  33. K. Meguellati, G. Korpelly and S. Ladame, *Angew. Chem. Int. Ed.*, 2010, **49**, 2738.
  34. (a) Y. Huang and J. M. Coull, *J. Am. Chem. Soc.*, 2008, **130**, 3238; (b) D. K. Prusty and A. Herrmann, *J. Am. Chem. Soc.*, 2010, **132**, 12197.
  35. G. Clavé, A. Bernardin, M. Massonneau, P.-Y. Renard and A. Romieu, *Tetrahedron Lett.*, 2006, **47**, 6229.
  36. G. Chen, D. J. Yee, N. G. Gubernator and D. Sames, *J. Am. Chem. Soc.*, 2005, **127**, 4544.
  37. J. Zhou, Y. Luo, Q. Li, J. Shen, R. Wang, Y. Xu and X. Qian, *New J. Chem.*, 2014, **38**, 2770.
  38. Z. Lei and Y. Yang, *J. Am. Chem. Soc.*, 2014, **136**, 6594.
  39. Y. Yang, S. K. Seidlits, M. M. Adams, V. M. Lynch, C. E. Schmidt, E. V. Anslyn and J. B. Shear, *J. Am. Chem. Soc.*, 2010, **132**, 13114.
  40. Y.-M. Shen, L.-L. Song, X.-H. Qian and Y.-J. Yang, *Chin. Chem. Lett.*, 2013, **24**, 7.
  41. Q. Zhang, Z. Zhu, Y. Zheng, J. Cheng, N. Zhang, Y.-T. Long, J. Zheng, X. Qian and Y. Yang, *J. Am. Chem. Soc.*, 2012, **134**, 18479.
  42. A. Rajapakse and K. S. Gates, *J. Org. Chem.*, 2012, **77**, 3531.
  43. For selected examples of bio-labile hemithioaminal and  $\alpha$ -alkoxy carbamate moieties, see: (a) Y. Meyer, J.-A. Richard, M. Massonneau, P.-Y. Renard and A. Romieu, *Org. Lett.*, 2008, **10**, 1517; (b) R. A. Mosey and P. E. Floreancig, *Org. Biomol. Chem.*, 2012, **10**, 7980; (c) E. L. Schneider, L. Robinson, R. Reid, G. W. Ashley and D. V. Santi, *Bioconjugate Chem.*, 2013, **24**, 1990.
  44. B. Ballou, L. A. Ernst and A. S. Waggoner, *Curr. Med. Chem.*, 2005, **12**, 795.
  45. D. M. Beal and L. H. Jones, *Angew. Chem. Int. Ed.*, 2012, **51**, 6320.



46. W. J. Smith, N. P. Oien, R. M. Hughes, C. M. Marvin, Z. L. Rodgers, J. Lee and D. S. Lawrence, *Angew. Chem., Int. Ed.*, 2014, **53**, 10495.
47. G. Liang, H. Ren and J. Rao, *Nat. Chem.*, 2010, **2**, 54.
48. (a) D. Ye, G. Liang, M. L. Ma and J. Rao, *Angew. Chem., Int. Ed.*, 2011, **50**, 2275; (b) A. Dragulescu-Andrasi, S.-R. Kothapalli, G. A. Tikhomirov, J. Rao and S. S. Gambhir, *J. Am. Chem. Soc.*, 2013, **135**, 11015; (c) A. Godinat, H. M. Park, S. C. Miller, K. Cheng, D. Hanahan, L. E. Sanman, M. Bogyo, A. Yu, G. F. Nikitin, A. Stahl and E. A. Dubikovskaya, *ACS Chem. Biol.*, 2013, **8**, 987; (d) D. Ye, P. Pandit, P. Kempen, J. Lin, L. Xiong, R. Sinclair, B. Rutt and J. Rao, *Bioconjugate Chem.*, 2014, **25**, 1526; (e) D. Ye, A. J. Shuhendler, L. Cui, L. Tong, S. S. Tee, G. Tikhomirov, D. W. Felsher and J. Rao, *Nat. Chem.*, 2014, **6**, 519; (f) D. Ye, A. J. Shuhendler, P. Pandit, K. D. Brewer, S. S. Tee, L. Cui, G. Tikhomirov, B. Rutt and J. Rao, *Chem. Sci.*, 2014, **5**, 3845; (g) Y. Yuan and G. Liang, *Org. Biomol. Chem.*, 2014, **12**, 865.
49. G. C. Van de Bittner, C. R. Bertozzi and C. J. Chang, *J. Am. Chem. Soc.*, 2013, **135**, 1783.
50. (a) W. Zhou, C. Andrews, J. Liu, J. W. Shultz, M. P. Valley, J. J. Cali, E. M. Hawkins, D. H. Klaubert, R. F. Bulleit and K. V. Wood, *ChemBioChem*, 2008, **9**, 714; (b) W. Zhou, D. Leippe, S. Duellman, M. Sobol, J. Vidugiriene, M. O'Brien, J. W. Shultz, J. J. Kimball, C. DiBernardo, L. Moothart, L. Bernad, J. Cali, D. H. Klaubert and P. Meisenheimer, *ChemBioChem*, 2014, **15**, 670.
51. (a) N. R. Conley, A. Dragulescu-Andrasi, J. Rao and W. E. Moerner, *Angew. Chem., Int. Ed.*, 2012, **51**, 3350; (b) S. T. Adams Jr and S. C. Miller, *Curr. Opin. Chem. Biol.*, 2014, **21**, 112.
52. For recent works about other far-red or NIR-emitting luciferin analogues, see: (a) A. P. Jathoul, H. Grounds, J. C. Anderson and M. A. Pule, *Angew. Chem., Int. Ed.*, 2014, **53**, 13059; (b) D. M. Mofford, G. R. Reddy and S. C. Miller, *J. Am. Chem. Soc.*, 2014, **136**, 13277; (c) M. C. Pirrung, G. Biswas, N. De Howitt and J. Liao, *Bioorg. Med. Chem. Lett.*, 2014, **24**, 4881.
53. L. C. Wang, D. S. Scherr and S. F. Shariat, in *Prostate Cancer Diagnosis - PSA, Biopsy and Beyond*, ed. J. S. Jones, Humana Press, New York, 2013, ch. 7, pp. 73.
54. A. Chevalier, Ph. D. DiSSERTATION, Université de Rouen, 2014.
55. (a) M. Ogawa, N. Kosaka, C. A. S. Regino, M. Mitsunaga, P. L. Choyke and H. Kobayashi, *Mol. BioSyst.*, 2010, **6**, 888; (b) H. Kobayashi, M. R. Longmire, M. Ogawa and P. L. Choyke, *Chem. Soc. Rev.*, 2011, **40**, 4626.
56. M. Prost and J. Hasserodt, *Chem. Commun.*, 2014, **50**, 14896.
57. For recent examples, see: (a) Q. Xu, K.-A. Lee, S. Lee, K. M. Lee, W.-J. Lee and J. Yoon, *J. Am. Chem. Soc.*, 2013, **135**, 9944; H. Sun, L. Yi, H. Zhang, C. Zhang and R. Liu, *Chem. Commun.*, 2014, in press, see DOI: 10.1039/C4CC08156K
58. For recent reviews about far-red or NIR single-analyte-responsive fluorescent probes, see: (a) L. Yuan, W. Lin, K. Zheng, L. He and W. Huang, *Chem. Soc. Rev.*, 2013, **42**, 622; (b) Z. Guo, S. Park, J. Yoon and I. Shin, *Chem. Soc. Rev.*, 2014, **43**, 16.
59. (a) N. Karton-Lifshin, E. Segal, L. Omer, M. Portnoy, R. Satchi-Fainaro and D. Shabat, *J. Am. Chem. Soc.*, 2011, **133**, 10960; (b) N. Karton-Lifshin, L. Albertazzi, M. Bendikov, P. S. Baran and D. Shabat, *J. Am. Chem. Soc.*, 2012, **134**, 20412; (c) E. Kisin-Finifer and D. Shabat, *Bioorg. Med. Chem.*, 2013, **21**, 3602.

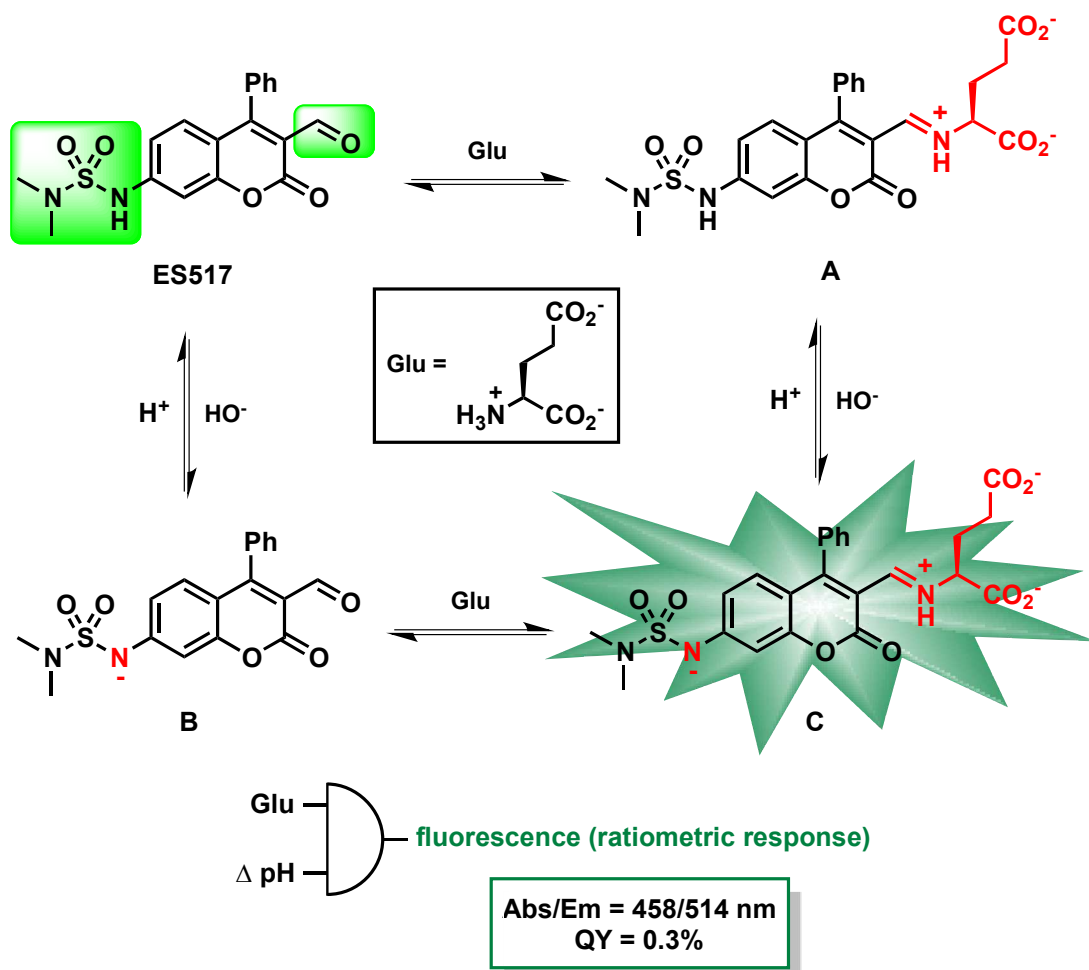


**Fig. 1** "AND" molecular logic gate for neuronal imaging based on the fluorogenic reaction of ES517 with two distinct analytes namely glutamate and hydroxide anion (ratiometric response).

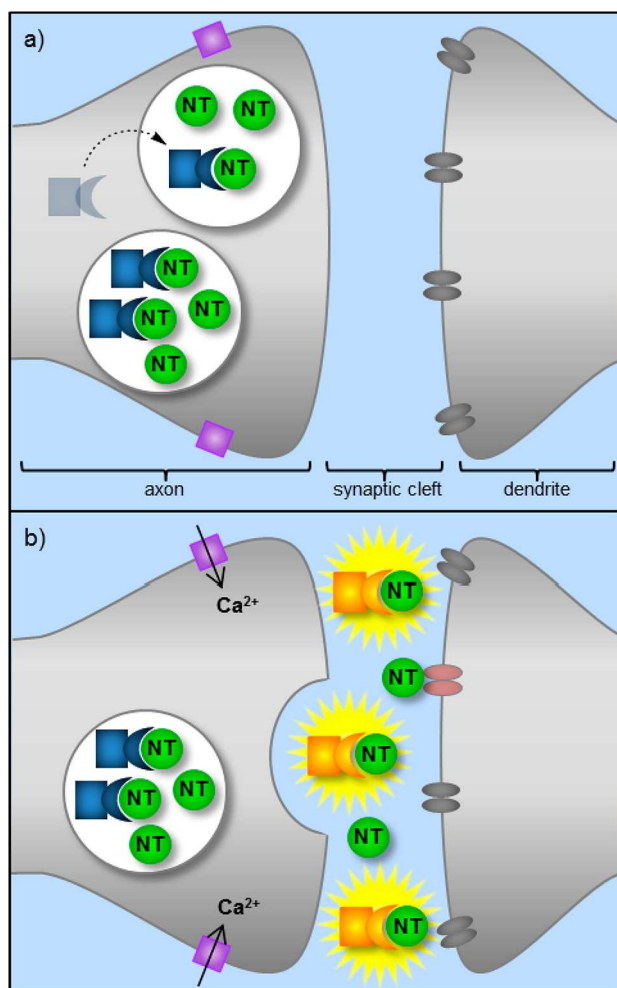


**Fig. 2** Sensing mechanism of ES517. (a) Sensor enters vesicle and selectively labels the neurotransmitter (NT). The bound complex accumulates and green fluorescence at 514 nm is "off" due to low pH (5). (b) Influx of Ca(II) triggers exocytosis. The increase in environmental pH in the synaptic cleft (7.4) switches the green fluorescence "on" for only the bound complex. Reproduced with permission from Klockow *et al.*<sup>19</sup>. Copyright 2013 American Chemical Society.

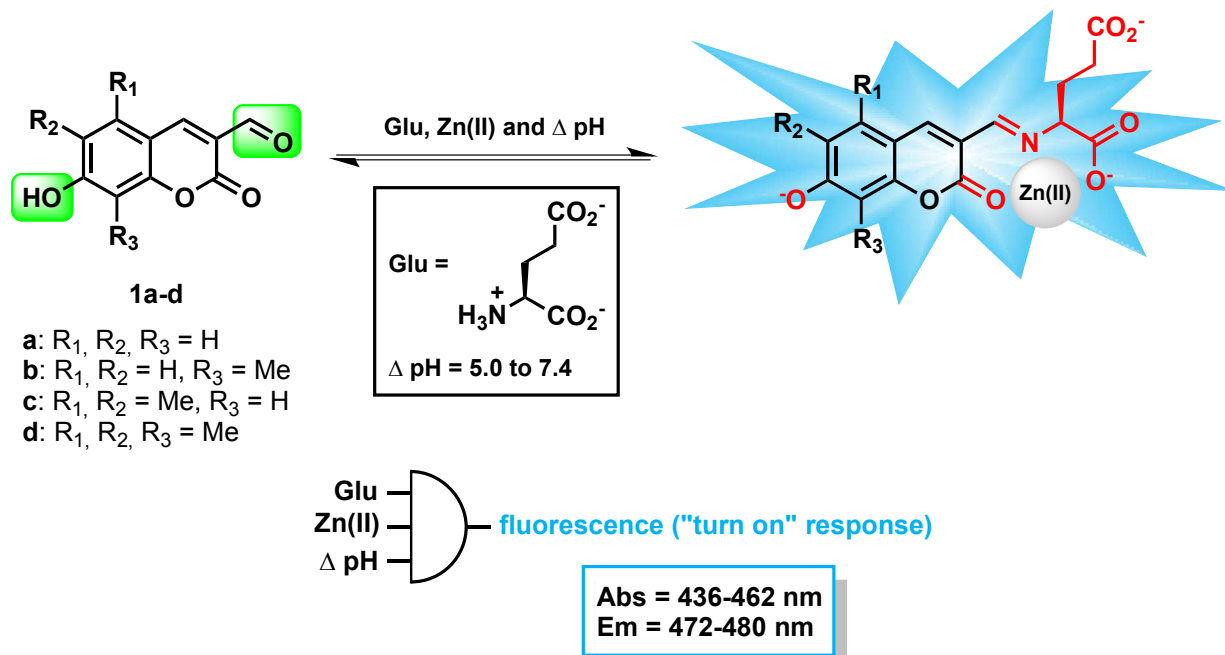


**Fig. 3** "AND" molecular logic gate for neuronal imaging based on the fluorogenic reaction of **1a-d** with three distinct analytes namely glutamate, Zn(II) cation and hydroxide anion ("turn-on" response).



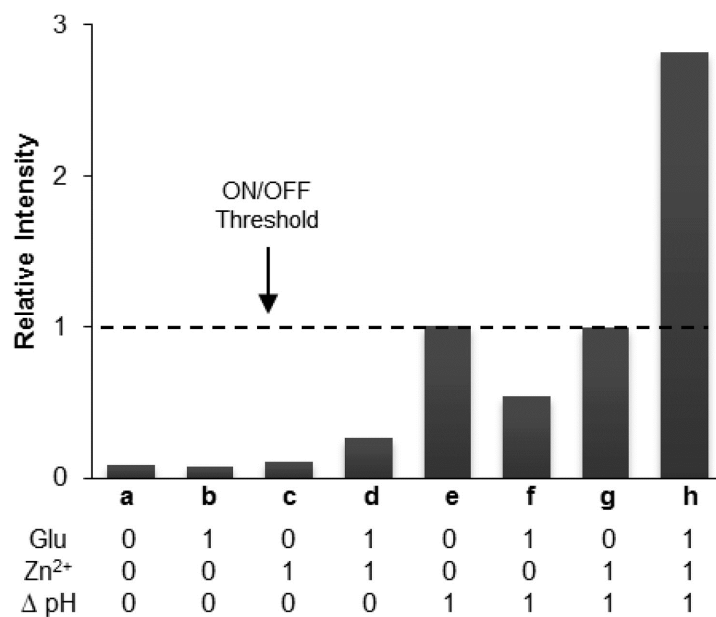


**Fig. 4** Relative fluorescence intensities and truth table for **1c**, a three-input "AND" fluorescent molecular logic gate. Samples contained **1c** (1  $\mu$ M) in buffer (50 mM HEPES, 120 mM NaCl, 1% DMSO) in the presence or absence of Glu (500 mM) and Zn(OAc)<sub>2</sub> (40 mM).  $\Delta$  pH = increase in pH from 5.0 to 7.4. Reproduced with permission from Hettie *et al.*<sup>20</sup>. Copyright 2014 American Chemical Society.

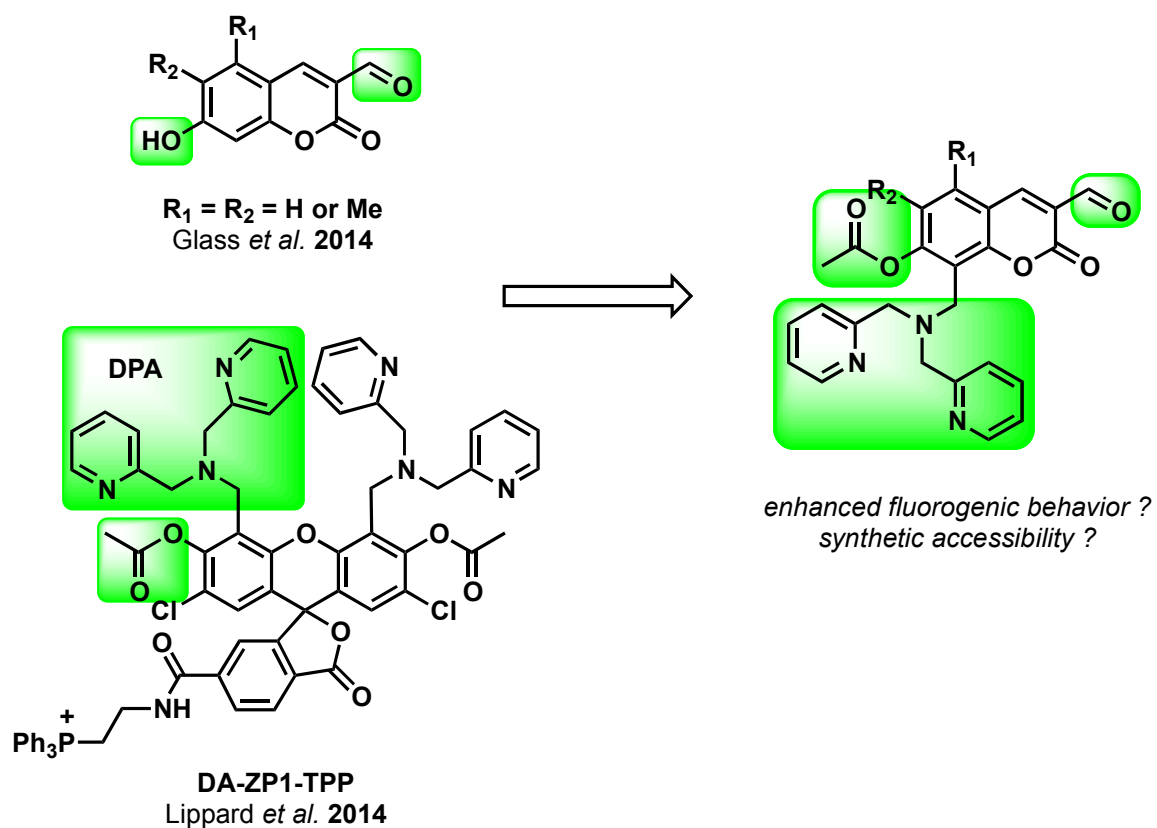
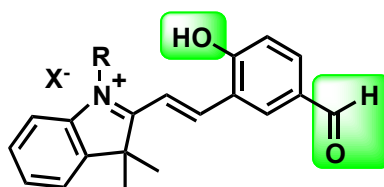


**Fig. 5** A possible way to improve the fluorogenic behavior of 7-hydroxycoumarin-based "AND" molecular logic gate, suitable for neuronal imaging.



*red-shifted Abs/Em maxima compared to  
3-formyl-7-hydroxycoumarin ?*

**Fig. 6** A suggested structure of latent fluorescent platform (derived from the core structure of NIR fluorogenic dyes recently developed by Shabat and co-workers<sup>59</sup>), to red-shift absorption/emission maxima of the three-input "AND" fluorescent molecular logic gate suitable for neuronal imaging.

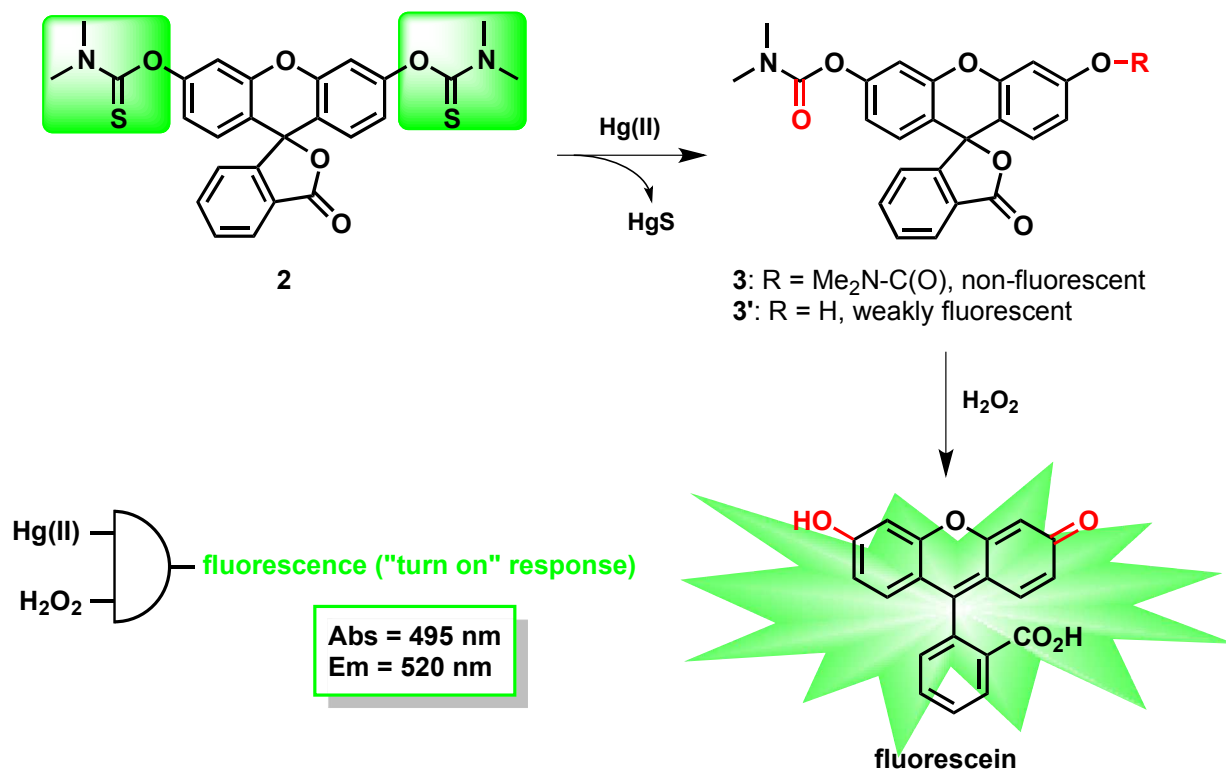


**Fig. 7** "AND" molecular logic gate based on the fluorogenic deprotection of bis-(dimethylthiocarbamate)-caged fluorescein **2** mediated sequentially by Hg(II) cation and H<sub>2</sub>O<sub>2</sub> ("turn-on" response).



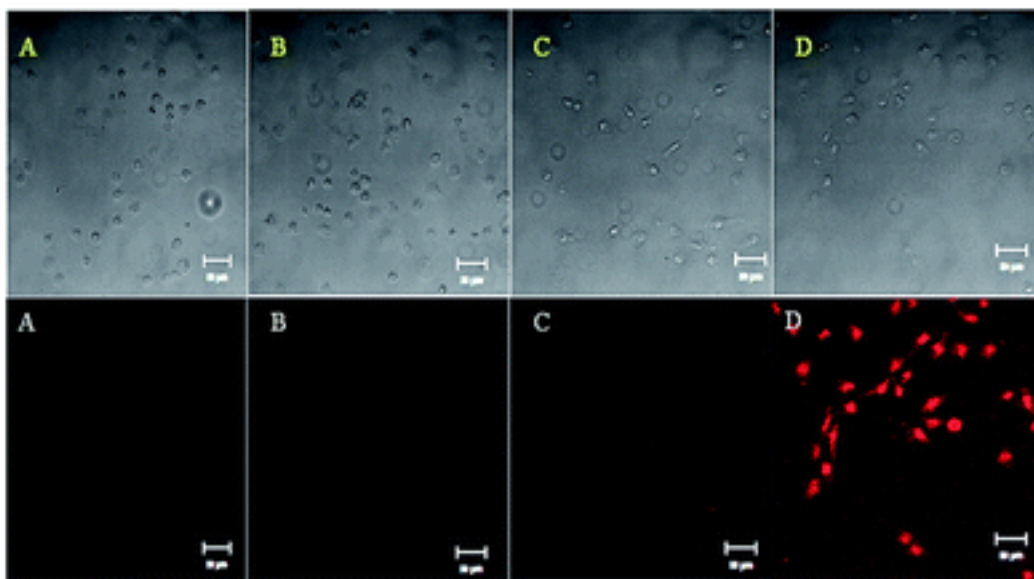


**Fig. 8** Fluorescence microscopy data: (upper) bright field images, (lower) fluorescence images, (A) control, (B) SH-SY5Y neuroblastoma cells with pro-fluorophore **2**, (C) cells with **2** and Hg(II), and (D) cells after incubation with **2** + Hg(II) + and H<sub>2</sub>O<sub>2</sub> for 1 h. Ex at 546 nm (scale bar = 50  $\mu$ m). Reproduced with permission from Murale *et al.*<sup>23</sup>. Copyright 2013 Royal Society of Chemistry.

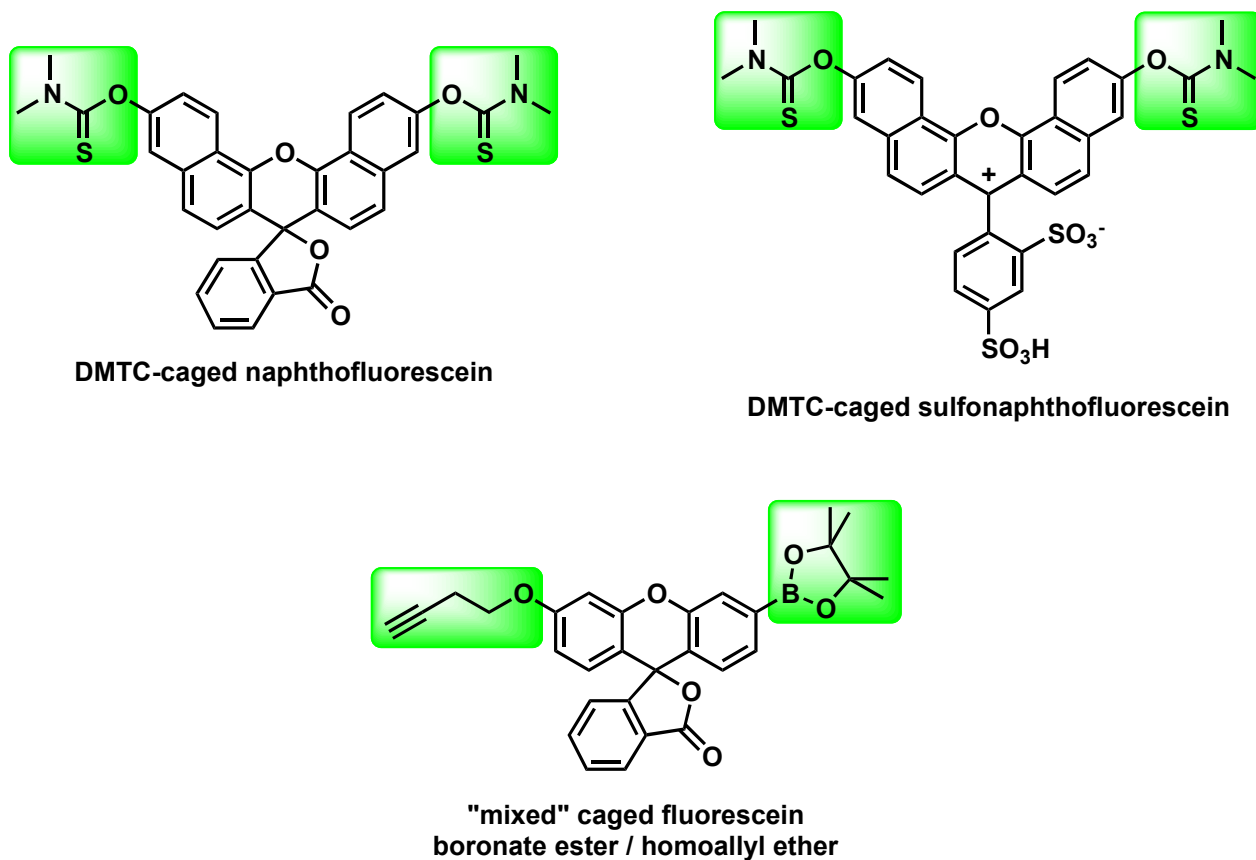


**Fig. 9** Possible ways to red-shift absorption/emission maxima (top) and to improve the selectivity (bottom) of the two-input "AND" fluorescent molecular logic gate suitable for tandem Hg(II) and H<sub>2</sub>O<sub>2</sub> chemosensing (DMTC = dimethylthiocarbamate).

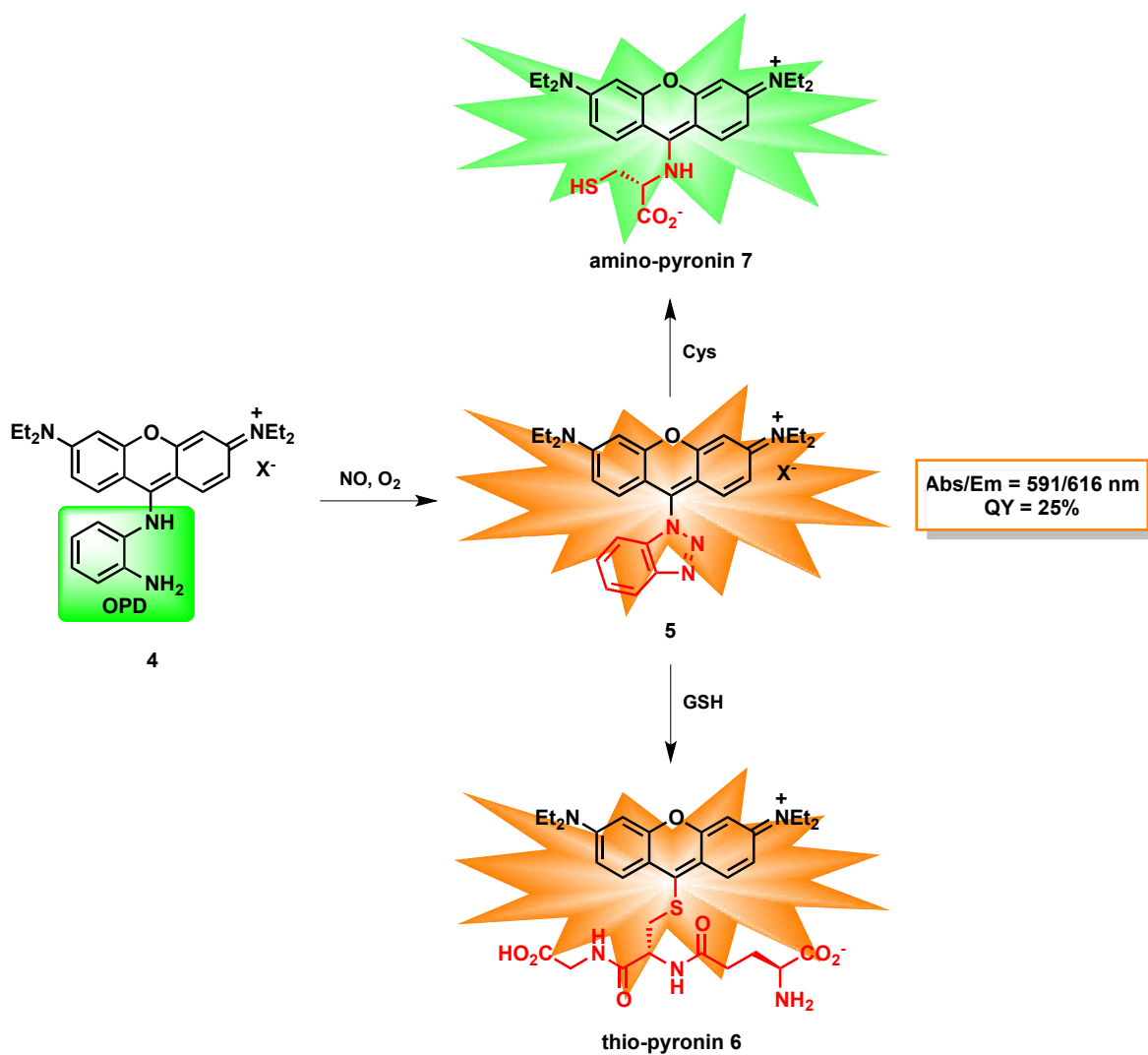


**Fig. 10** Fluorescent probe OPD-pyronin B 4 for dual-channel nitric oxide (NO) imaging assisted by intracellular biothiols (Cys or GSH). Fluorogenic reaction mechanism proposed by Guo and co-workers<sup>27</sup>.

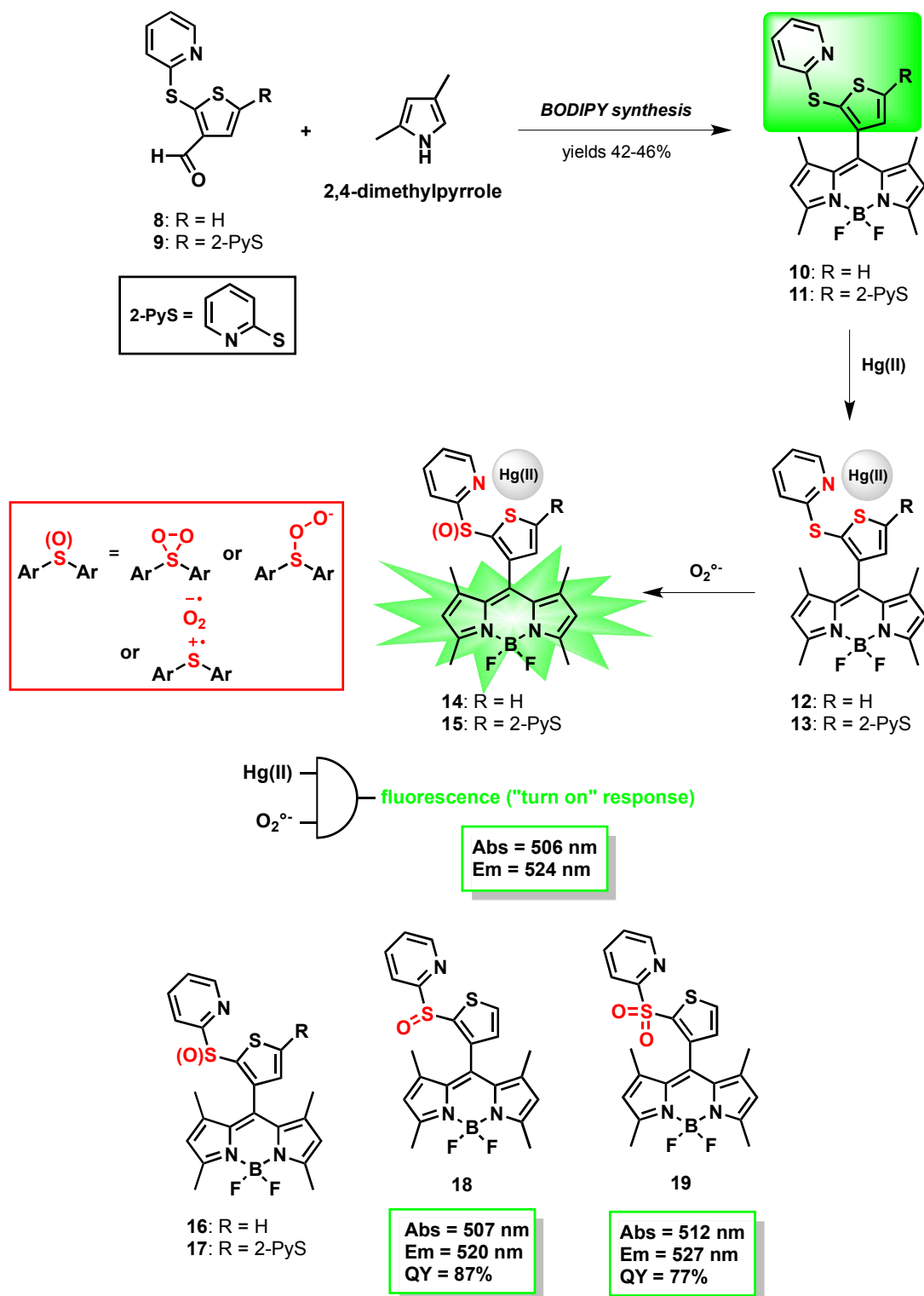


**Fig. 11** "AND" molecular logic gate based on the fluorogenic metal-chelation/oxidation process of BODIPY-based probes **10** and **11**, mediated by Hg(II) cation and superoxide anion radical  $O_2^{\cdot-}$  ("turn-on" response).



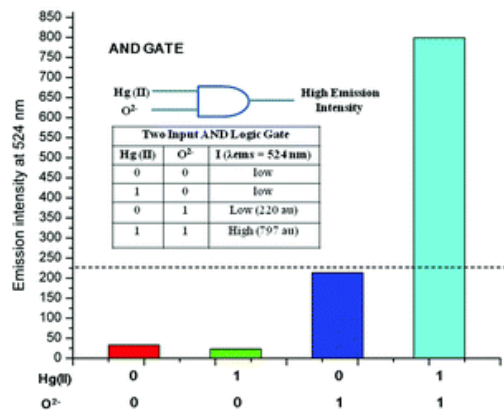


**Fig. 12** Relative fluorescence intensities and truth table for **11**, a two-input "AND" fluorescent molecular logic gate. Samples contained **11** (1  $\mu$ M) in buffer CH<sub>3</sub>CNH<sub>2</sub>O (7 : 3, v/v) in the presence or absence of Hg(II) (18 equiv) and O<sub>2</sub><sup>-</sup> (18 equiv). Reproduced with permission from Singh *et al.*<sup>28</sup>. Copyright 2013 Royal Society of Chemistry.

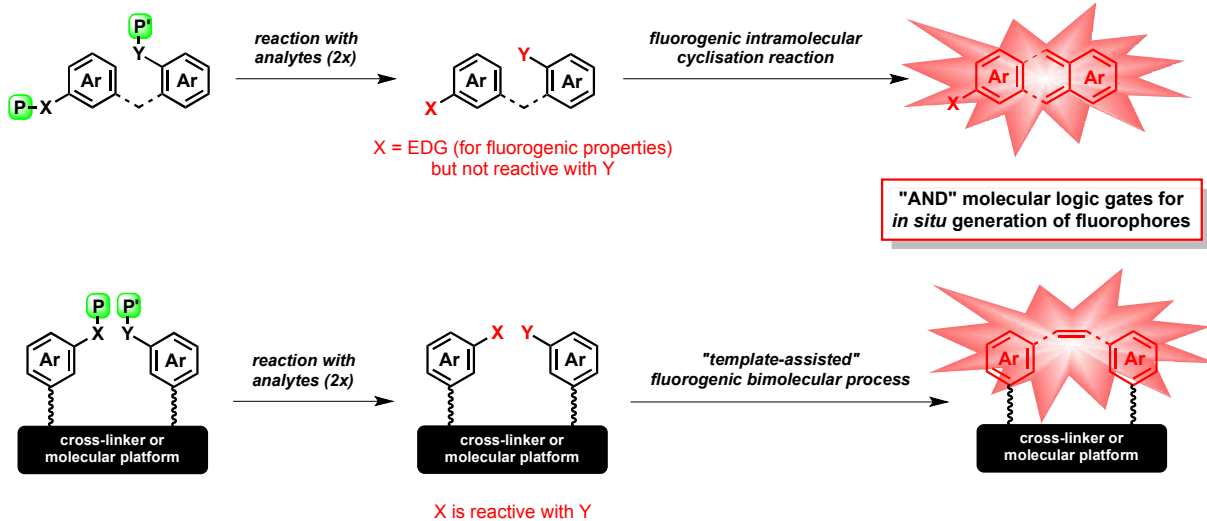


**Fig. 13** "AND" fluorescent molecular logic gate based on cascades of covalent bond-modifying reactions triggered by two distinct (bio)analytes: (top) *in situ* generation of a fluorophore through an intramolecular cyclisation reaction triggered by one of the two (bio)analytes (the second one acts as a deprotection reagent for fluorogenic reactive site X, EDG = electron-donating group); (bottom) *in situ* assembly of a fluorophore from two caged precursors whose functional reactive groups X and Y are released through specific reactions with the target (bio)analytes.

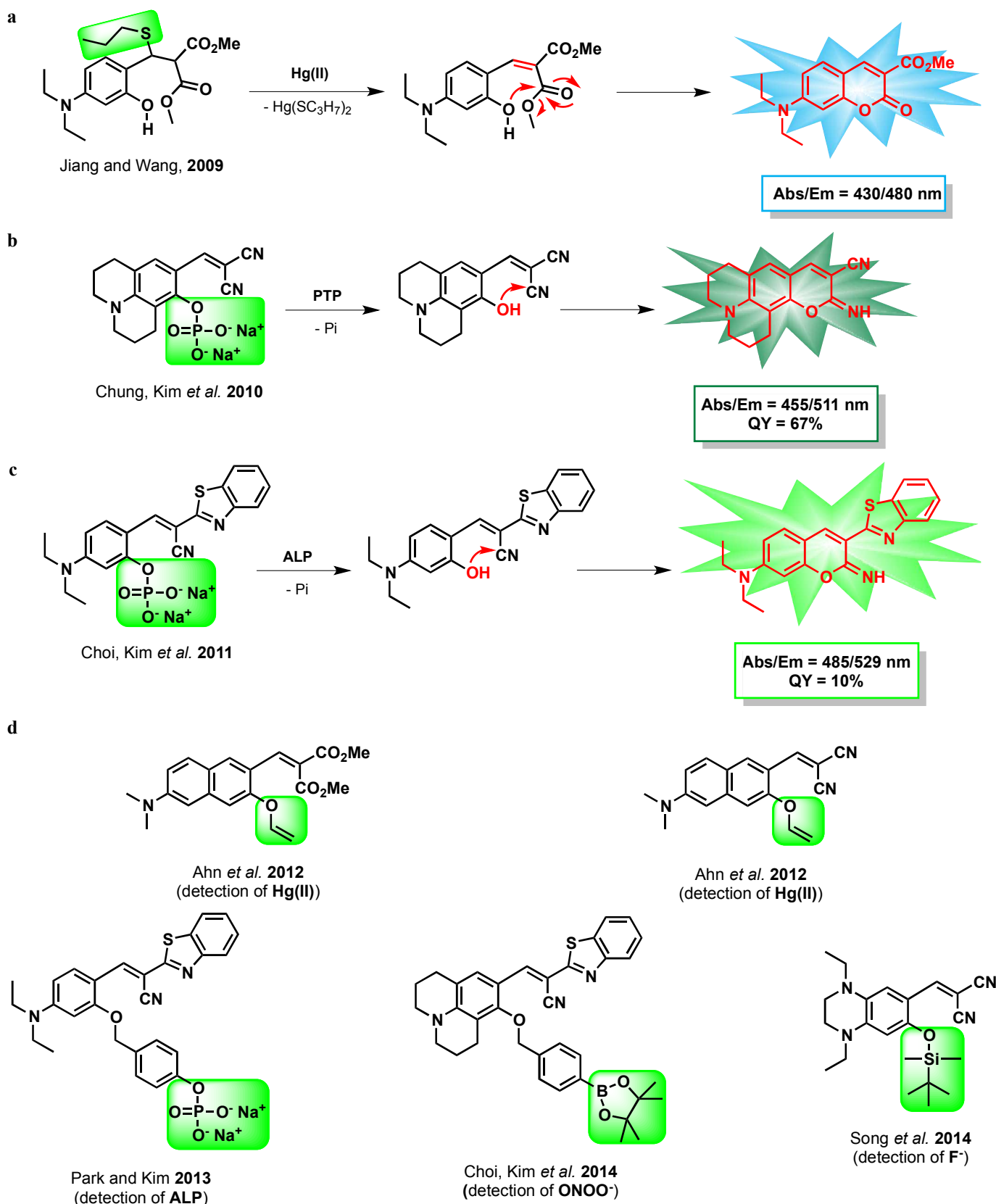


**Fig. 14** "Turn-on" fluorescent (bio)analyte sensing based on *in situ* formation of (imino)coumarin scaffolds. PTP = protein tyrosine phosphatase, ALP = alkaline phosphatase, Pi = phosphate anion.

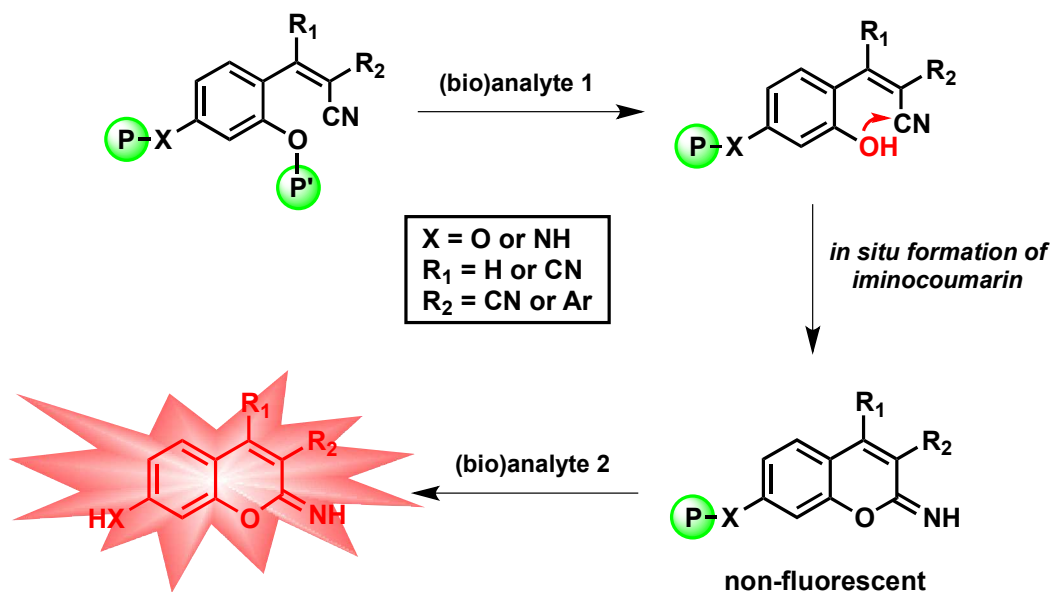


**Fig. 15** "AND" fluorescent molecular logic gate based on *in situ* formation of a free 7-amino/7-hydroxycoumarin scaffold mediated by two distinct (bio)analytes (by analogy with formalism used in Figure 13, O = Y): an intramolecular cyclisation reaction triggered by one of the two (bio)analytes and subsequent aniline/phenol deprotection induced by the second one.

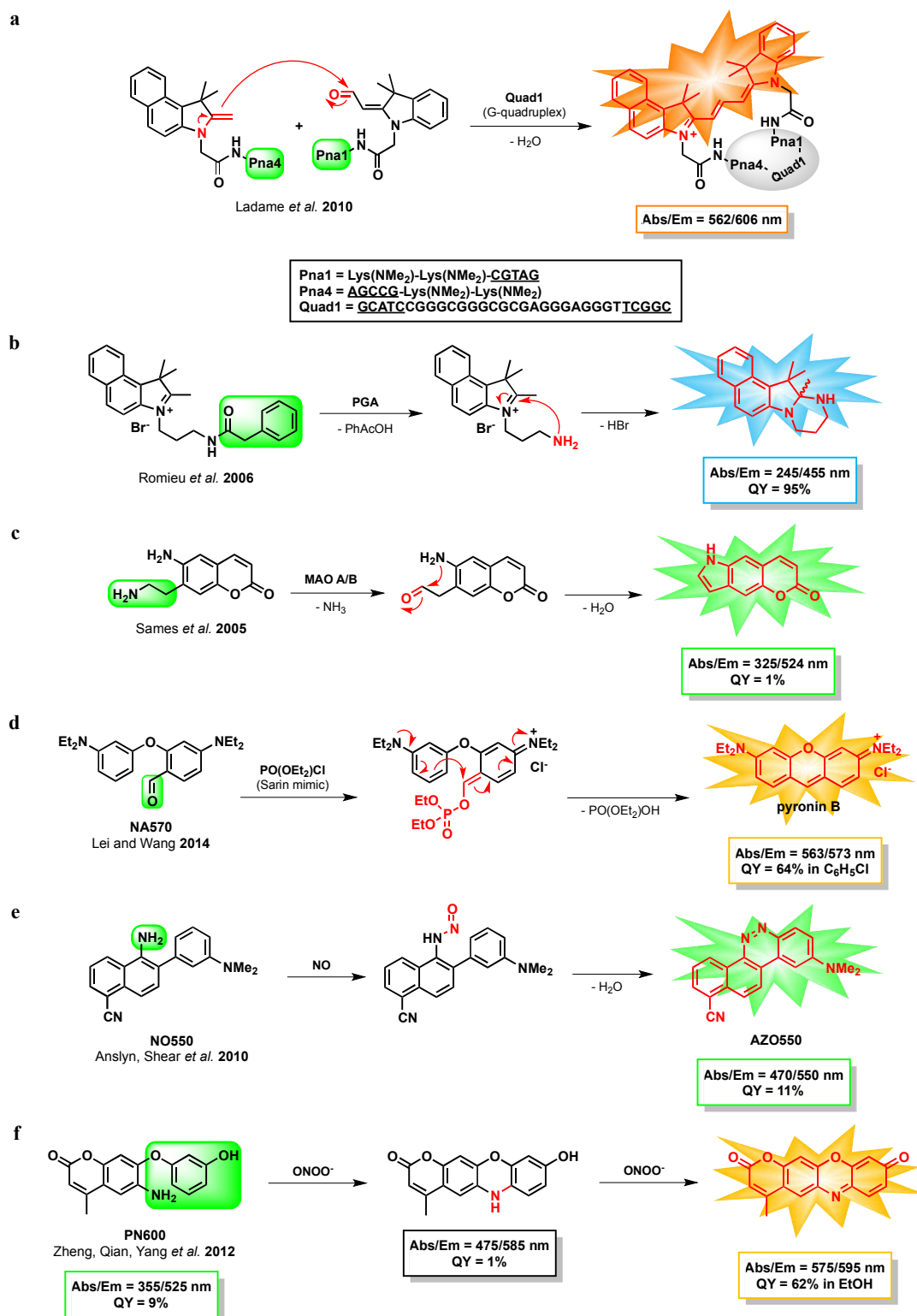


**Fig. 16** Fluorogenic reactions triggered by a single (bio)analyte and leading to *in situ* formation of a fluorophore scaffold. (a) Aldolisation-elimination reaction<sup>33</sup>; (b) Mannich cyclisation<sup>35</sup>; (c) intramolecular addition-elimination reaction<sup>36</sup>; (d) phenylogous Vilsmeier-Haack reaction<sup>38</sup>; (e) cascade reaction: nitrosation, S<sub>E</sub>Ar and dehydration<sup>39</sup>; (f) tandem phenol oxidation-Michael addition<sup>41</sup>. The reported quantum yield values (QY) were determined in water (or related aq. buffers), unless stated otherwise.

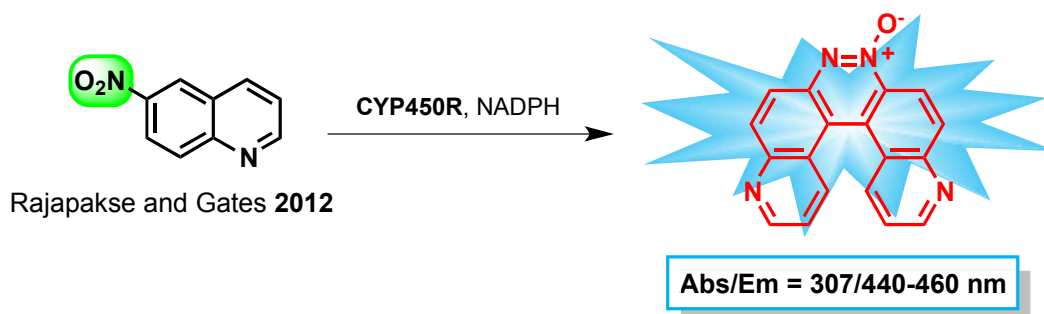


**Fig. 17** An unusual example of fluorogenic reaction triggered by a reductase (CYP450R = cytochrome P450 reductase) and leading to the conversion of 6-nitroquinoline into a fluorescent helicene named pyrido[3,2-*f*]quinolino[6,5-*c*]cinnoline 3-oxide. For a possible mechanism for the formation of this azoxyhelicene, see ref.<sup>42</sup>.



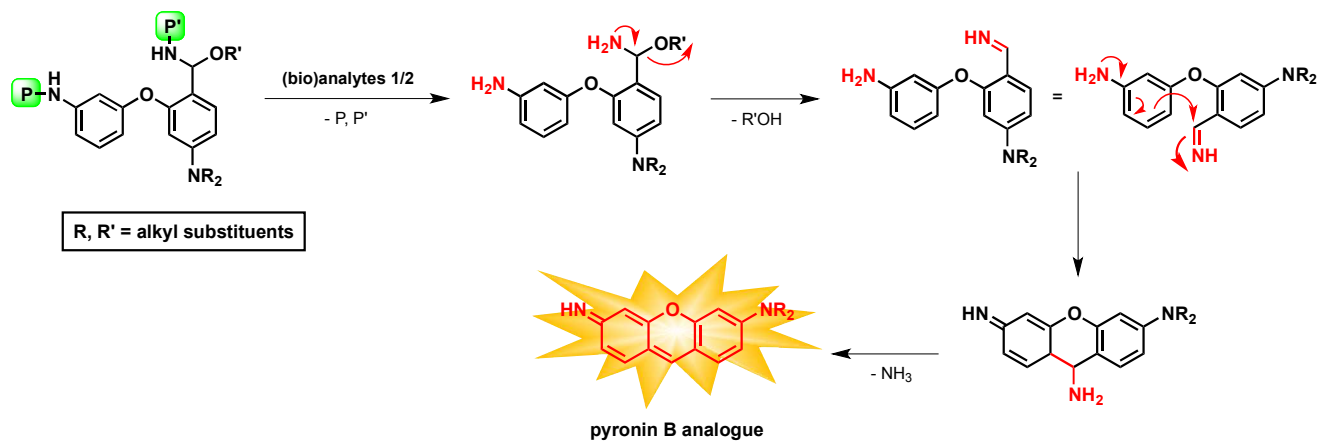


**Fig. 18** One possible strategy for the simultaneous detection of two distinct (bio)analytes through "covalent assembly" approach: *in situ* formation of an unsymmetrical pyronin fluorophore (P and P' = carboxamide or carbamate protecting groups). Please note that the intermediate imine can be hydrolysed to aldehyde but a similar intramolecular cyclisation reaction can take place to provide unsymmetrical pyronin fluorophore (elimination of a water molecule).

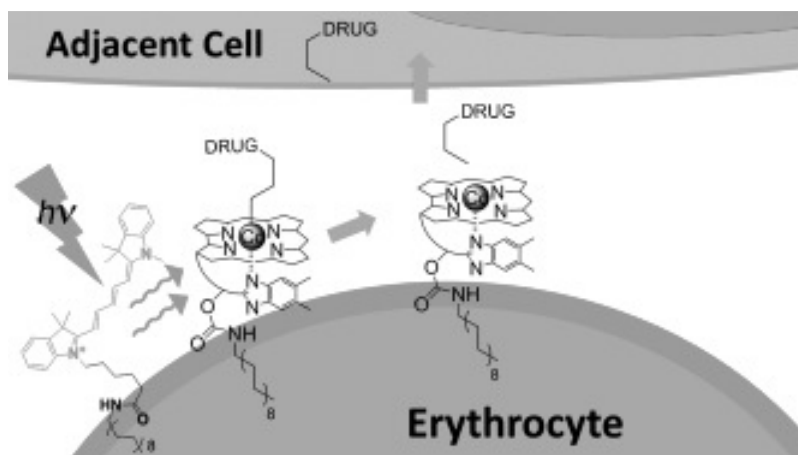


**Fig. 19** A wavelength-encoded drug-release strategy. Anti-inflammatory drugs are covalently appended to cobalamin (Cbl) by means of a photolabile Co-C bond. Lipidated-Cbl and fluorophore constructs assemble on the plasma membrane of human erythrocytes. The fluorophore serves as an antenna, capturing long-wavelength light and transmitting the energy to the Cbl-drug conjugate, resulting in drug release from the erythrocyte carrier. Reproduced with permission from ref.<sup>46</sup>. Copyright 2014 JohnWiley & Sons, Inc.

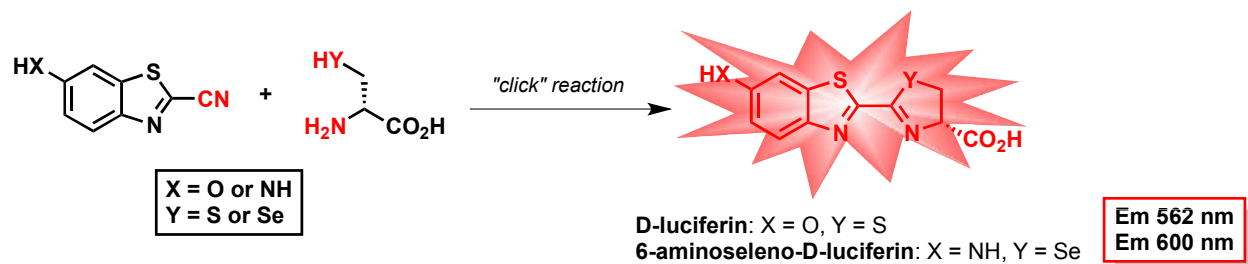


**Fig. 20** The "click" reaction between free D-(seleno)cysteine and 6-amino/6-hydroxy CBT derivative, for the synthesis of D-luciferin (or 6-aminoseleno-D-luciferin).

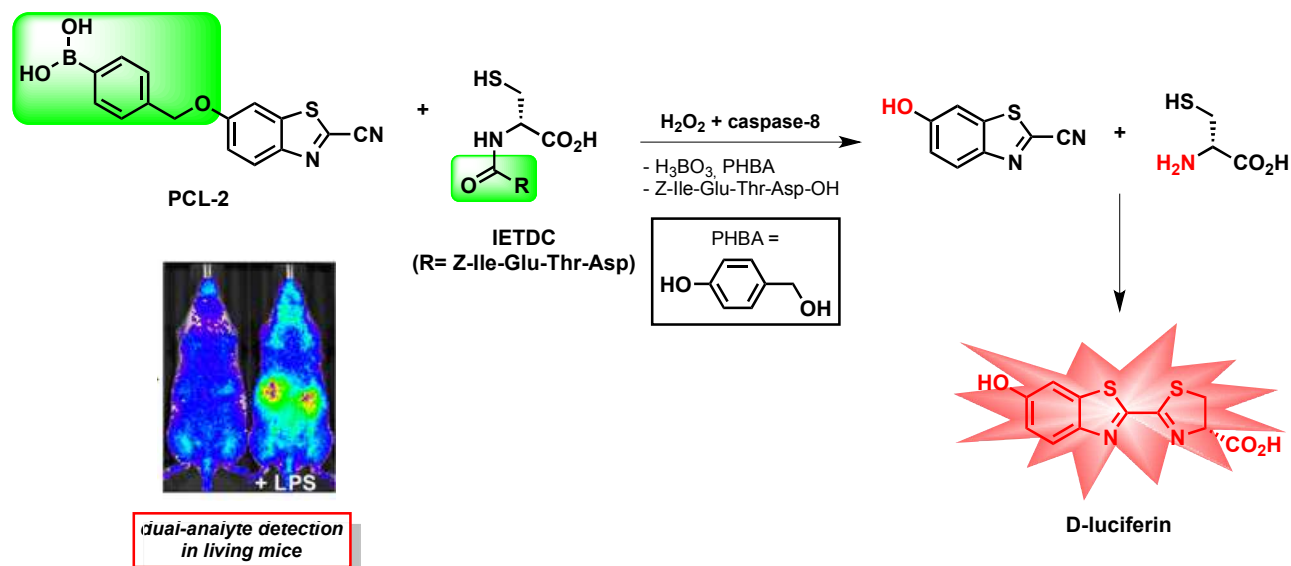
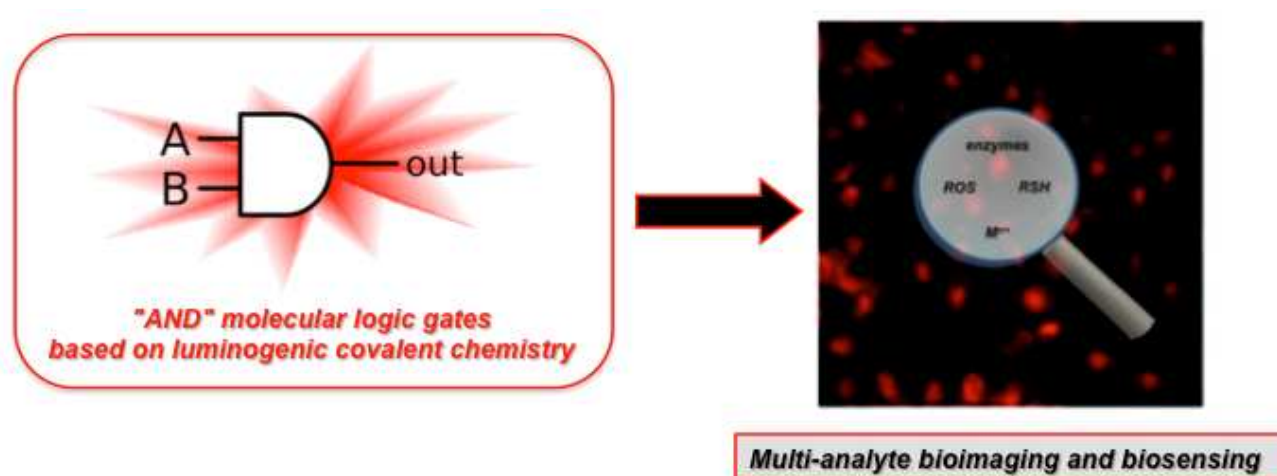


**Fig. 21** "Self-assembly" bioluminogenic approach for dual-analyte luciferin imaging: *in vivo* bioluminescence detection of  $\text{H}_2\text{O}_2$  and caspase-8 in a murine model of acute inflammation (LPS = lipopolysaccharides used to induce an acute inflammatory response). Bioluminescent images reproduced with permission from ref.<sup>49</sup>. Copyright 2013 American Chemical Society.

## Table of Content

**"AND" luminescent "reactive" molecular logic gates: a gateway to multi-analyte bioimaging and biosensing**

Anthony Romieu



This feature article focuses on the recent development of "AND" luminescent molecular logic gates, in which the optical output is produced in response to multiple (bio)chemical inputs and through cascades of covalent bond-modifying reactions triggered by target (bio)analytes. This emerging class of "smart" optical bioprobes is an alternative to conventional "AND" molecular logic gates based on supramolecular photochemical mechanisms, particularly for biosensing and bioimaging applications in complex media.



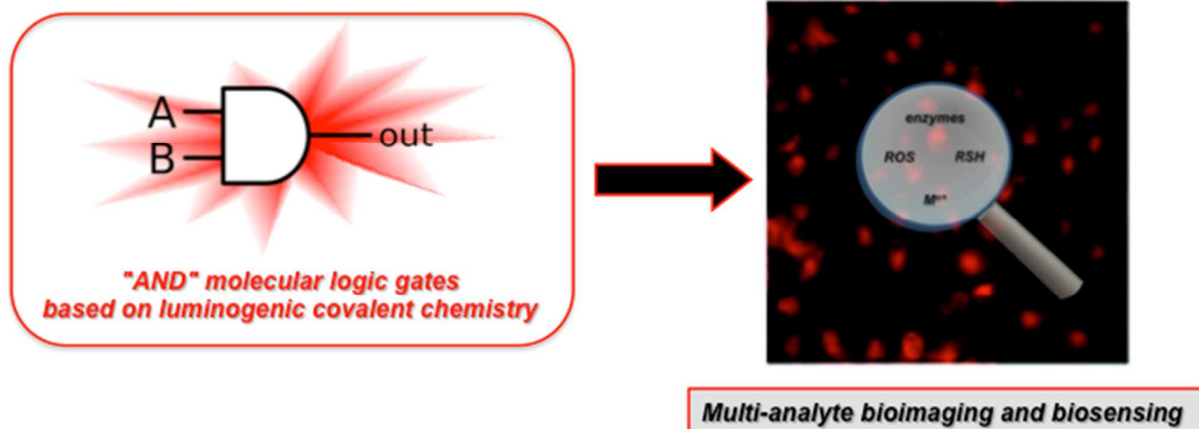
**Anthony Romieu** obtained his Ph. D. from the University Josph Fourrier (Grenoble, France) under the guidance of Drs. Jean Cadet and Didier Gasparutto (Laboratory of Nucleic Acids Damages, CEA-Grenoble) in 1999. After a two-year experience as CNRS study engineer in the lab of Pr. B.-P. Roques at the University Paris 5, in the fields of medicinal chemistry and peptide synthesis, he joined in june 2001 the private biotech company Manteia Predictive Medicine (spin-off of the Serono group, Switzerland) as a senior scientist in bioorganic chemistry. The core buisness of this company was devoted to the development and commercialisation of an original high-throughput DNA sequencing technology. Following a restructuring leading to the acquisition of Manteia by Solexa Ltd. (this latter company will become a wholly owned subsidiary of Illumina, Inc. in january 2007), he has been appointed as lecturer in bioorganic chemistry at the University of Rouen. From february 2004 to august 2013, he co-facilitated with Pr. P.-Y. Renard the bioorganic chemistry research team from the COBRA lab (UMR CNRS 6014). In september 2013, he was appointed as full professor at the University of Burgundy and member junior of the French University Institute (IUF). He also joined the ICMUB lab (UMR CNRS 6302) and his current research interests mainly focus on the development of advanced chemical tools ("smart" optical (bio)probes, novel fluorogenic reactions, cross-linking reagents for multiple bioconjugation) for biosensing and bioimaging applications. He is co-author of 70 scientific papers and co-inventor of over a dozen of patents, three of them are being actively pursued by Illumina company (Genome Analyzer DNA sequencing technology).



## Table of Content

**"AND" luminescent "reactive" molecular logic gates: a gateway to multi-analyte bioimaging and biosensing**

Anthony Romieu



This feature article focuses on the recent development of "AND" luminescent molecular logic gates, in which the optical output is produced in response to multiple (bio)chemical inputs and through cascades of covalent bond-modifying reactions triggered by target (bio)analytes. This emerging class of "smart" optical bioprobes is an alternative to conventional "AND" molecular logic gates based on supramolecular photochemical mechanisms, particularly for biosensing and bioimaging applications in complex media.